Uniqueness of integer lattice point constellations in $\mathbb{Z}^7$

Philippe A.J.G. Chevalier

De oogst 7, B-9800 Deinze, Belgium

Abstract

The constellations of lattice points are important in information theory. We study constellations of lattice points forming parallelograms in the *seven* dimensional integer lattice $\mathbb{Z}^7$. The distribution of the parallelogram perimeters displays frequencies with a value $f = 1$ that indicates the existence of *unique constellations*. We discover that the unique constellations are embedded in specific hyperplanes of the integer lattice $\mathbb{Z}^7$. We find that the measure polytopes P_7^s with edge length $2s$, where $s = \ell_\infty$ is the Chebyshev norm, are the framework for the classification of the parallelogram perimeter distributions. We demonstrate that the mathematical structure S classifying the distributions is based on *leader classes* which are distinct constellations of integer lattice points, that are related through a signed permutation of the integer lattice point coordinates. The appendices contain a preliminary classification of the distributions based on the measure polytope P_7^{10} and also numerical data useful as starting point for the further exploration of the integer lattice point constellations.

Keywords: centrally symmetric polytope, lattice polytope, isoperimeter, 7-dimensional integer lattice
2010 MSC: 52B12, 52B20, 52B60, 52C07

1. Introduction

We use as mathematical framework a 7-dimensional integer lattice $\mathbb{Z}^7$.

1.1. Outline of the paper

1.2. Preliminaries

Let the set of integer septuples $\mathbb{Z}^7 \doteq \{(X^1, \ldots, X^7) \mid X^i \in \mathbb{Z}\}$ be called the 7-dimensional integer lattice. A set of lattice points is called a *lattice constellation* [25]. The A^is are the contravariant components of the lattice point $\breve{a}$. The Abelian group $\mathbb{Z}^7$ [26] is a $\mathbb{Z}$-module. The family $\{\mathbb{Z}, \mathbb{Z}^2, \mathbb{Z}^3, \mathbb{Z}^4, \mathbb{Z}^5, \mathbb{Z}^6\}$ are $\mathbb{Z}$-submodules of $\mathbb{Z}^7$. The $\mathbb{Z}$-module $\mathbb{Z}^7/\mathbb{Z}$ is called the quotient module of $\mathbb{Z}^7$ with respect to $\mathbb{Z}$. The prerequisite for the creation of a vector space is the existence of a field $\mathbb{F}$ for the scalars. The elements of the vector space are then vectors. This justifies the notation $\breve{a}$, indicating that the elements of $\mathbb{Z}^7, +, \cdot$ are *not* vectors $\boldsymbol{a}$. We select 7 linearly independent lattice points $\breve{e}_1, \ldots, \breve{e}_7$ of $\mathbb{Z}^7$. The $\breve{e}_i$s form a covariant basis [27] for the integer lattice in $\mathbb{Z}^7$. Every lattice point is expressed in a unique way as the linear combination: $\breve{x} = X^1\breve{e}_1 + \ldots + X^7\breve{e}_7$ where the

Email address: `chevalier.philippe.ajg@gmail.com` (Philippe A.J.G. Chevalier)

coefficients X^i are called the contravariant components of $\breve{x}$. The inner product is defined as the expression: $\breve{x}\cdot\breve{y}=\sum_{i=1}^{7}\sum_{j=1}^{7}a_{ij}X^iY^j$ where $a_{ij}=a_{ji}$. Consider seven lattice points $\breve{e}^i$ satisfying the expression $\breve{e}^i=\sum_{k=1}^{7}a^{ik}\breve{e}_k$. This contravariant basis spans the space $\mathbb{Z}^7$ resulting in the equations $\sum_{i=1}^{7}a_{ij}\breve{e}^i=\sum_{i=1}^{7}\sum_{k=1}^{7}a_{ij}a^{ik}\breve{e}_k=\sum_{k=1}^{7}\delta_j^k\breve{e}_k=\breve{e}_j$. A lattice point $\breve{x}$ has covariant components X_i, such that $\breve{x}=\sum_{i=1}^{7}X_i\breve{e}^i$. These components are related to the contravariant components by the expressions: $X^j=\sum_{i=1}^{7}a^{ij}X_i$ and $X_i=\sum_{i=1}^{7}a_{ij}X^j$. With this notation the inner product is represented as $\breve{x}\cdot\breve{y}=\sum_{i=1}^{7}X^iY_i=\sum_{k=1}^{7}X_kY^k$. Observe that, since $\breve{e}^i\cdot\breve{e}_j=\sum_{i=1}^{7}a^{ik}\breve{e}_k\cdot\breve{e}_j=\sum_{i=1}^{7}a^{ik}a_{jk}=\delta_j^i$, each $\breve{e}^i$ is orthogonal to every $\breve{e}_j$ except $\breve{e}_i$. We obtain that $\breve{e}^i\cdot\breve{e}_j=1$. We are free to select seven basis lattice points. We define: $\breve{l}\doteq\breve{e}_1=(1,0,0,0,0,0,0)$, $\breve{m}\doteq\breve{e}_2=(0,1,0,0,0,0,0)$, $\breve{t}\doteq\breve{e}_3=(0,0,1,0,0,0,0)$, $\breve{i}\doteq\breve{e}_4=(0,0,0,1,0,0,0)$, $\breve{T}\doteq\breve{e}_5=(0,0,0,0,1,0,0)$, $\breve{n}\doteq\breve{e}_6=(0,0,0,0,0,1,0)$, $\breve{L}\doteq\breve{e}_7=(0,0,0,0,0,0,1)$, with $\breve{e}_i\in\mathbb{Z}^7$. This basis generates a *cubic lattice* [29] that is orthonormal. We call the expression $N(\breve{x})\doteq\|\breve{x}\|_1=\sum_{i=1}^{7}\sum_{k=1}^{7}a_{ik}X^iX^k$, the ℓ_1-norm of $\breve{x}$ in $\mathbb{Z}^7$. We call the expression $\|\breve{x}\|_2\doteq\sqrt{\sum_{i=1}^{7}\sum_{k=1}^{7}a_{ik}X^iX^k}$ the ℓ_2-norm or Euclidean norm of $\breve{x}$ in $\mathbb{Z}^7$. We call the expression $\|\breve{x}\|_\infty=max\{|X^1|,\ldots,|X^7|\}$ the Chebyshev norm or infinity norm of $\breve{x}$ in $\mathbb{Z}^7$. Let $\breve{x},\breve{y}$ be lattice points of $\mathbb{Z}^7$. The ℓ_2-distance (Euclidean distance) between the points $\breve{x},\breve{y}$ is defined by: $d(\breve{x},\breve{y})=\|\breve{x}-\breve{y}\|_2=\sqrt{\sum_{i=1}^{7}(X_i-Y_i)(X^i-Y^i)}$ where $\breve{x}-\breve{y}=(X^1-Y^1,\ldots,X^7-Y^7)$ if $\breve{x}=(X^1,\ldots,X^7)$ and $\breve{y}=(Y^1,\ldots,Y^7)$. We call two integer lattice points *neighbours* if their ℓ_2-distance is 1. We assign to each lattice point $\breve{x}$ of $\mathbb{Z}^7$ a hyperplane $H_{\breve{x}}$. A set $H_{\breve{x}}$ in $\mathbb{Z}^7$ is a hyperplane [30] if and only if there exist scalars $C_0,C_1,\ldots,C_7$, where not all $C_1,\ldots,C_7$ are zero, such that $H_{\breve{x}}=\{(X^1,\ldots,X^7)\mid C_0+C_1X^1+\ldots+C_7X^7=0\}$. Consider now the lattice point $\breve{y}=(Y^1,\ldots,Y^7)$ and select its associated hyperplane $H_{\breve{y}}$ that contains the lattice point $\breve{o}$. The lattice point $\breve{x}$ is incident on the hyperplane $H_{\breve{y}}$ when it satisfies the equation $\sum_{i=1}^{7}Y^iX_i=0$. The distance between the lattice point $\breve{z}$ and the hyperplane $H_{\breve{y}}$, measured along the perpendicular, is the projection of $\breve{o}\breve{z}$ in the direction of $\breve{o}\breve{y}$ that is given by the equation $\frac{\breve{z}\cdot\breve{y}}{\|\breve{y}\|_2}=\frac{\sum_{i=1}^{7}Z_iY^i}{\sqrt{\sum_{i=1}^{7}Y_iY^i}}$. Let the lattice point $\breve{x}'$ be the image of $\breve{x}$ by reflection in the hyperplane $H_{\breve{y}}$. Consider the lattice point $\breve{z}$ satisfying $\breve{z}=\breve{x}-\breve{x}'$, then the line $\breve{o}\breve{z}$ is parallel to the line $\breve{o}\breve{y}$. We define now a general reflection [27] in the hyperplane $H_{\breve{y}}$ as $\breve{x}-\breve{x}'=2\frac{\breve{x}\cdot\breve{y}}{\breve{y}\cdot\breve{y}}\breve{y}$. We call the lattice point $\breve{y}$ the *root* [31] of the reflecting hyperplane $H_{\breve{y}}$. The root system for the Lie algebra B_7 [32] has the basis $\breve{\alpha}_1,\ldots,\breve{\alpha}_7$ defined by $\breve{\alpha}_1=\breve{e}_1-\breve{e}_2,\ \breve{\alpha}_2=\breve{e}_2-\breve{e}_3,\ \ldots,\breve{\alpha}_6=\breve{e}_6-\breve{e}_7,\ \breve{\alpha}_7=\breve{e}_7$. This root system generates the $\mathbb{Z}^7$ integer lattice as root lattice [31] by reflections in the hyperplanes associated with the roots. The reflections are characterized by *signed permutation matrices* [32]. As we will connect points in the integer lattice, we use the term *path* from graph theory [33], where a k-path is a simple graph of length k, i.e., consisting of k vertices and k edges and represented by a sequence of consecutive vertices $\breve{x}_0 \dots \breve{x}_{k-1}$ [33]. The Euclidean dimension of a graph G is the smallest integer p such that the vertices of G can be represented by points in the Euclidean space $\mathbb{Z}^p$ with two points being 1 unit distance apart if and only if they represent adjacent vertices [34]. For undefined terms from graph theory see [33].

Definition 1. Let the surjective function "psc", represent the *parity of the sum of coordinates* of a lattice point of $\mathbb{Z}^7$ and define:

$$\text{psc} : \mathbb{Z}^7 \to \{0, 1\} \mid \text{psc}\,(\breve{x}) = |\sum_{i=1}^{7} X^i| \pmod 2 \,, X^i \in \mathbb{Z} \,.$$

The "psc" function is a 2-colouring function. We have an *evensum* lattice point when $\text{psc}\,(\breve{x}) = 0$ and an *oddsum* lattice point when $\text{psc}\,(\breve{x}) = 1$ where $\breve{x} \in \mathbb{Z}^7$. Observe that the lattice points $\breve{x}$ for which $\text{psc}\,(\breve{x}) = 0$ are elements of D_7 that is an indecomposable root lattice [35] defined as $D_7 = \{(X^1, \dots, X^7) \in \mathbb{Z}^7 \mid \sum_{i=1}^{7} X^i \; \textit{is even}\}$. The lattice D_7 has 84 minimal points, that are $\pm\breve{e}_j \pm \breve{e}_k$ where $(1 \leq j < k \leq 7)$. These 84 points form a simple basis derived from the canonical basis $\breve{e}_1, \dots, \breve{e}_7$ of $\mathbb{Z}^7$. Consider a lattice point $\breve{x}_0$ and points $\breve{x}$, which have the property $\breve{x}_0 + \breve{x} \in A \Leftrightarrow \breve{x}_0 - \breve{x} \in A$ then we call A a centrally symmetric set. In the remainder of the article we will assume that $\breve{x}_0 = \breve{o}$ is the origin of $\mathbb{Z}^7$. An *integer lattice polytope* is the convex hull of a set of finitely many points in $\mathbb{Z}^d$. A measure polytope P_d^s of edge-length $2s$ is a subset of $\mathbb{Z}^d$ with the following property $P_d^s = \{\breve{x}(X^1, \dots, X^d) \in \mathbb{Z}^d \mid \|\breve{x}\|_\infty = s\}$, where $X^i \in \mathbb{Z}$ and $(1 \leq i \leq d)$.

2. Parallelogram as constellation of lattice points

The 4-cycle $\breve{o}\breve{y}\breve{z}\breve{x}\breve{o}$ is equal to *circuit*($\breve{o}\breve{y}\breve{z}\breve{x}\breve{o}$) where the constellation *oyzxo* describes a hamiltonian circuit. Let the parallelogram *oyzxo* represent a directed graph on the vertices $1, \dots, 4$ and let the variable u_i denote the vertex that follows vertex i in the sequence. The set of values that u_i can take is the set of integers j for which (i, j) is an edge of the parallelogram *oyzxo*. The constraint *circuit*(u_1, u_2, u_3, u_4) requires that $u = (u_1, u_2, u_3, u_4)$ describes a hamiltonian circuit, and thus u is a circuit if $\pi_1, \dots, \pi_n$ is a permutation of $1, \dots, n$, where $\pi_1 = 1$ and $\pi_{i+1} = u_{\pi_i}$ for $i = 1, \dots, (n-1)$ [36]. Thus $\pi_1, \dots, \pi_n$ indicates the order in which the vertices are visited.

3. Cardinality of isoperimetric parallelograms

We explore the integer lattice and search for constellation where the elements of the constellation are forming a parallelogram $\breve{o}\breve{y}\breve{z}\breve{x}\breve{o}$. The followed approach was to select two fixed points $\breve{o}, \breve{z}$ and to vary the point $\breve{x}$ and derive the coordinates of the lattice point $\breve{y}$. For ease of calculation perimeters of triangles p_t instead of parallelograms p_p were calculated and then converted. The fixed point to start the survey through the integer lattice was selected to be $\breve{z} = (2, 1, -2, 0, 0, 0, 0)$. The question became now more specific: Which lattice points are generating triangles representing an *energy* constellation between physical quantities and how many of these triangles have the same perimeter? Two polygons are called *isoperimetric* [37] if they have the same perimeter. A program in MATLAB® was first created, but rapidly computational/memory problems occurred due to the large amount of data to be processed. The program was adapted and written in the programming language *C#*. The algorithm is given in appendix A. The absolute frequency of occurrence of these parallelogram perimeters p_p are tabulated as a sequence of non-negative integers and represented graphically for $\breve{z} = \breve{E}$, as a *discrete value distribution*[38]. We observed that the constellations representing energy are connected through the discrete value distribution in such a way that the frequency f is identical to the order n of a graph G of *vertices* representing *relations between physical quantities* and *edges* representing *a connection between relations of physical quantities.* This approach is similar to the one followed by Wigner where the *laws of nature* are the entities to which *the symmetry laws* apply [4].

3.1. Perimeter of a triangle

Let p_t be the perimeter of the triangle formed by the 3-cycle $\breve{o}\breve{z}\breve{x}\breve{o}$. The value of the perimeter p_t is obtained by the formula $p_t = \sqrt{u} + \sqrt{v} + \sqrt{w}$ with $u, v, w \in \mathbb{Z}_+$ and expressed through the following equations:

$$u = \sum_{i=1}^{7} x_i^2 \qquad v = \sum_{i=1}^{7} (x_i - z_i)^2 \qquad w = \sum_{i=1}^{7} z_i^2 \ .$$

3.2. Area of a triangle

Let A_t be the enclosed area of a triangle formed by the 3-cycle $\breve{o}\breve{z}\breve{x}\breve{o}$. The area of the triangle defined by the lattice points $\breve{o}\breve{z}\breve{x}$ is given by the equation, see Abramowitz and Stegun [39], $A_t = \frac{1}{2}hb$, where h is the height of the triangle which correponds to the distance from the lattice point $\breve{x}$ to the axis $\breve{o}\breve{z}$ and b is the base of the triangle and corresponds to $\|\breve{z}\|_2$. We call ϕ the angle between $\breve{z}$ and $\breve{x}$. From elementary goniometry, see Abramowitz and Stegun [39], we have:

$$cos^2(\phi) + sin^2(\phi) = 1 = \frac{(\sum_{i=1}^{7} z_i x_i)^2 + h^2 \|\breve{z}\|_2^2}{\|\breve{x}\|_2^2 \|\breve{z}\|_2^2} = \frac{(\sum_{i=1}^{7} z_i x_i)^2 + 4A_t^2}{\|\breve{x}\|_2^2 \|\breve{z}\|_2^2} \tag{1}$$

We rewrite the equation (1) to a quadratic form $Q(\breve{x})$

$$Q(\breve{x}) = (\sum_{i=1}^{7} z_i^2)(\sum_{i=1}^{7} x_i^2) - (\sum_{i=1}^{7} z_i x_i)^2 = 4A_t^2 \ ,$$

which is easily transformed to a matrix equation given by:

$$Q(\mathsf{X}) = \mathsf{X}^{tr}\mathsf{M}\mathsf{X} = 4A_t^2 = A_p^2 \ ,$$

and where X^{tr} is a 1×7 matrix, M is a symmetric 7×7 matrix and X is a 7×1 matrix. The term A_p^2 is the square of the area of the parallelogram formed by the 4-cycle $\breve{o}\breve{y}\breve{z}\breve{x}\breve{o}$. Observe that the quadratic form $Q(\mathsf{X})$ represents positive integers. The square of the area of the parallelogram has the property $A_p^2 \geq 1$, when degenerated parallelograms are excluded. The parallelogram for which $A_p^2 = 1$ is a fundamental parallelogram of $\mathbb{Z}^7$. Observe that the parallelograms have the lattice points $\breve{o}$ and $\breve{z}$ as foci of an ellipse E_a that has the lattice points $\breve{x}$ and $\breve{y}$ incident of it. From the definition of an ellipse we have $2a = \sqrt{u} + \sqrt{v}$.

3.3. Case study for the physical quantity energy

The lattice point $\breve{z} = (2, 1, -2, 0, 0, 0, 0) = \breve{E}$ represents the physical quantity *energy.* The graphical representation (Fig. 1) of the discrete value distribution of parallelogram perimeters p_p for parallelograms representing equations between physical quantities in $\mathbb{Z}^7$ resulting in the physical quantity *energy* shows a rich structure. It reveals the *distribution of energy constellations.* The enumeration as class 6 (Table F.12) of the first 50 frequencies is not found in the OEIS database [40]. Observe that the lowest frequency f_{min} in Fig. 1 for the *non-degenerated* parallelograms is $f_{min} = 1$ with exception of the point with perimeter $p_p = 6$, that is a degenerated parallelogram. This isoperimetric distribution shows that *unique* non-degenerated parallelograms exist, that form *unique constellations* between physical quantities. At perimeter $p_p = 7,657$ we find the well-known equation $E = \gamma m_0 c^2$ represented in its generic form as $E = \kappa_3 m_0 v^2$ (Table 1). Observe (Table 1) that the parity of the sum of the coordinates of the lattice points $\breve{x}$ are *odd* while those of the lattice points $\breve{y}$ are *even.* The components of physical quantities which are unknown to the author are marked U_i in the equations of components of physical quantities resulting in the physical quantity energy. The first row represents a degenerated parallelogram. The dimensionless quantity κ_1 is associated to the dimensionless quantity γ from the special relativity theory. The second row is recognized as the product of the linear momentum and the velocity. The third row is recognized as the kinetic energy and if $v = c$, as the famous equation $E = \gamma m_0 c^2$. The fourth column gives the inner product of $\breve{x}$ and $\breve{y}$. Observe that the lattice points $\breve{x}$ and $\breve{y}$ are *orthogonal* for $E(1, 3, 1)$. Thus, the well-known equation $E = \gamma m_0 c^2$ is a *rectangle.* We show later in section 6 the importance of this property of a parallelogram. The fourth row is a well-known form appearing as a term in a Hamiltonian. The other rows express constellations between physical quantities that are unknown to the author.

3.3.1. Graphs of order n=1

We use the notation $E(n, g, v)$ for identifying the separate energy constellations. The index n represents the order of the graph, the index g identifies the graph and the index v represents the vertex number in the graph.

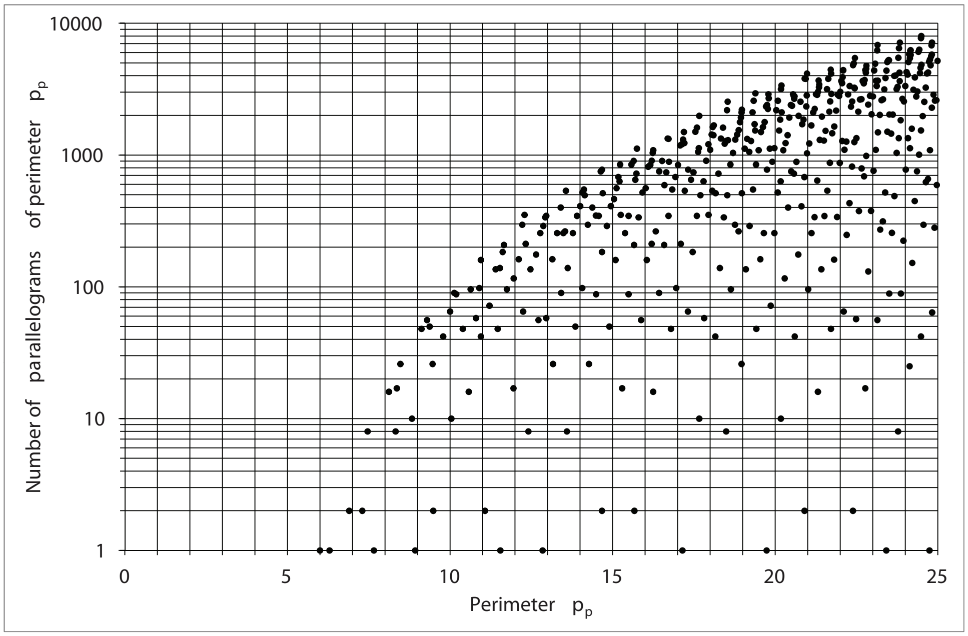

Figure 1: Discrete value distribution of parallelogram perimeters p_p in $\mathbb{Z}^7$ resulting in the physical quantity *energy*.

Table 1: Graphs of order $n = 1$ for *energy*.

n	g	v	p_p	$\breve{x}$	$\breve{y}$	$\breve{x} \cdot \breve{y}$	form
1	1	1	6,000	(2,1,-2,0,0,0,0)	(0,0,0,0,0,0,0)	0	$E(1,1,1) = \kappa_1 E_0$
1	2	1	6,293	(1,1,-1,0,0,0,0)	(1,0,-1,0,0,0,0)	2	$E(1,2,1) = \kappa_2 \boldsymbol{p} \cdot \boldsymbol{v}$
1	3	1	7,657	(0,1,0,0,0,0,0)	(2,0,-2,0,0,0,0)	0	$E(1,3,1) = \kappa_3 m_0 v^2$
1	4	1	8,928	(0,-1,0,0,0,0,0)	(2,2,-2,0,0,0,0)	-2	$E(1,4,1) = \kappa_4 \dfrac{p^2}{m_0}$
1	5	1	11,546	(3,1,-3,0,0,0,0)	(-1,0,1,0,0,0,0)	-6	$E(1,5,1) = \kappa_5 U_1 U_2$
1	6	1	12,845	(-1,-1,1,0,0,0,0)	(3,2,-3,0,0,0,0)	-8	$E(1,6,1) = \kappa_6 U_3 U_4$
1	7	1	17,146	(4,1,-4,0,0,0,0)	(-2,0,2,0,0,0,0)	-16	$E(1,7,1) = \kappa_7 \dfrac{U_5}{v^2}$
1	8	1	19,734	(4,3,-4,0,0,0,0)	(-2,-2,2,0,0,0,0)	-22	$E(1,8,1) = \kappa_8 \dfrac{U_6}{p^2}$
1	9	1	23,415	(-3,-1,3,0,0,0,0)	(5,2,-5,0,0,0,0)	-32	$E(1,9,1) = \kappa_9 U_7 U_8$
...	...	...	...	...	...	...	...

n	g	v	p_p	$\breve{x}$	$\breve{y}$	$\breve{x}\cdot\breve{y}$	form
1	10	1	24,743	(5,3,-5,0,0,0,0)	(-3,-2,3,0,0,0,0)	-36	$E(1,10,1) = \kappa_{10}U_9U_{10}$

The distribution in Fig. 1 is truncated at $p_p = 25$ due to edge effects at the hypercube surface. The edge effects are related to the memory capacity of the author's computer. The computation of the distribution in $\mathbb{Z}^7$ was performed for a Chebyshev norm $\|\breve{x}\|_\infty = 5$. The analysis covers 524287 parallelograms. The connectivity of the graphs is represented by $n = f = 1$ that is a single vertex having a loop. The loop, which is an edge, is represented by a 7×7 signed permutation matrix that transforms the relations in itself and so we find for the permutation matrix $\mathsf{P}_{11} = \mathsf{I}_7$. The signed permutation matrices π are $\mathbb{Z}$-linear maps for which $\pi\breve{o} = \breve{o}$ and $\pi(-\breve{a}) = -\pi\breve{a}$ for all $\breve{a} \in \mathbb{Z}^7$. Observe in Fig. 2 that all the unique *energy* equations are embedded in $\mathbb{Z}^3 \times \{0\}^4$ and localized in the hyperplane $H_{\breve{a}} = \{(X^1,\ldots,X^7) \mid X^1 + X^3 = 0\}$ with $\breve{a} = (1,0,1,0,0,0,0)$ that represents the product of *length* and *time*. We know that this product is a relativistic invariant in the special relativity theory. Observe in Fig. 2 the symmetry axes determined by the line containing *origin* and *energy* and the line containing *velocity* and *linear momentum*. We calculated the squared area A_p^2 of each parallelogram and find for the graphs of order $n = f = 1$ the equation $\log_2(A_p^2) = 2k+1$ with $k \in \mathbb{Z}_+$.

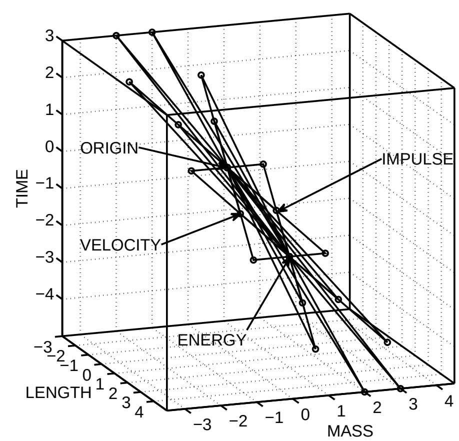

Figure 2: Unique parallelograms resulting in the physical quantity *energy*.

Let $x_i = \dfrac{1}{\kappa_i}$ with i = 1 to 10. The set $X = \{x_1,\ldots,x_{10}\}$ represents 10 dimensionless physical variables $x_i \in \mathbb{R}$ that are constructed from graphs of order 1.

Example 3.1. $x_1 = \dfrac{E_0}{E},\ x_2 = \dfrac{\boldsymbol{p}\cdot\boldsymbol{v}}{E},\ x_3 = \dfrac{m_0v^2}{E},\ x_4 = \dfrac{p^2}{m_0E},\ldots$

We define a monomial $x^\alpha = \prod_{i=1}^{10} x_i^{\alpha_i}$ where $\alpha = (\alpha_1,\ldots,\alpha_{10})$ is a 10-tuple of non-negative integers. We form a finite linear combination of monomials x^α to obtain a multivariate polynomial f. The set of all multivariate polynomials in $x_1,\ldots,x_{10}$ with coefficients in $\mathbb{R}$ is denoted

$\mathbb{R}[x_1,\ldots,x_{10}]$ [41]. Let $f_1,\ldots,f_s$ be multivariate polynomials in $\mathbb{R}[x_1,\ldots,x_{10}]$ then we define $\mathbf{V}(f_1,\ldots,f_s)=\{(x_1,\ldots,x_{10})\in\mathbb{R}^{10}\mid f_i(x_1,\ldots,x_{10})=0\}$ for all $1\le i\le s$. We call $\mathbf{V}(f_1,\ldots,f_s)$ the affine variety defined by $f_1,\ldots,f_s$ [41].

Example 3.2. $\mathbf{V}(x_2^2+x_3^2-1)$, that describes a unit circle in $\mathbb{R}^2$, is the variety that represents the states of a free particle of rest mass m_0, after the assignment $v=c$ in the dimensionless variable x_3.

The further elaboration on the construction of other varieties based on dimensionless variables is beyond the scope of the present article.

3.3.2. Graphs of order n=2

We analyse the parallelograms in Fig. 1 having frequency $f=2$. The result is given in the Table 2. Components of physical quantities which are *unknown* to the author are marked U_j. The first and second row in Table 2 represent two equations. The first equation is recognized as Planck's equation $E=\kappa_1 h\nu$, when the angular momentum $J=h$. The second equation $W=\kappa_2\int \boldsymbol{F}\cdot d\boldsymbol{s}$ represents the work done by the force $\boldsymbol{F}$. Both equations are combined to a new constellation described by the form $\kappa_2\int \boldsymbol{F}\cdot d\boldsymbol{s}=\kappa_1 h\nu$.

Table 2: Graphs of order $n=2$ for *energy.*

n	g	v	p_p	$\breve{x}$	$\breve{y}$	$\breve{x}\cdot\breve{y}$	form
2	1	1	6,899	(0,0,-1,0,0,0,0)	(2,1,-1,0,0,0,0)	1	$E(2,1,1)=\kappa_1 J\omega$
2	1	2	6,899	(1,0,0,0,0,0,0)	(1,1,-2,0,0,0,0)	1	$E(2,1,2)=\kappa_2 Fs$
2	2	1	7,301	(2,0,-1,0,0,0,0)	(0,1,-1,0,0,0,0)	1	$E(2,2,1)=\kappa_3\frac{\partial A}{\partial t}\frac{\partial m}{\partial t}$
2	2	2	7,301	(1,0,-2,0,0,0,0)	(1,1,0,0,0,0,0)	1	$E(2,2,2)=\kappa_4 aU_1$
2	3	1	9,483	(-1,0,0,0,0,0,0)	(3,1,-2,0,0,0,0)	-3	$E(2,3,1)=\kappa_5\frac{U_2}{r}$
2	3	2	9,483	(0,0,1,0,0,0,0)	(2,1,-3,0,0,0,0)	-3	$E(2,3,2)=\kappa_6 Pt$
2	4	1	11,075	(3,2,-2,0,0,0,0)	(-1,-1,0,0,0,0,0)	-5	$E(2,4,1)=\kappa_7 U_3U_4$
2	4	2	11,075	(2,2,-3,0,0,0,0)	(0,-1,1,0,0,0,0)	-5	$E(2,4,2)=\kappa_8\frac{U_5}{\frac{m}{t}}$

The signed 7×7 permutation matrix $\mathsf{P}_{211,212}$ that transforms *all* the relations of the graphs of order 2 is:

$$\mathsf{P}_{211,212}=\begin{bmatrix}0&0&-1&0&0&0&0\\0&1&0&0&0&0&0\\-1&0&0&0&0&0&0\\0&0&0&1&0&0&0\\0&0&0&0&1&0&0\\0&0&0&0&0&1&0\\0&0&0&0&0&0&1\end{bmatrix}$$

The matrix $\mathsf{P}_{211,212}$ has the property of being a symmetric matrix. Observe that the permutation matrix $\mathsf{P}_{211,212}$ has a block diagonal structure:

$$\mathsf{P}_{211,212} = \begin{bmatrix} \mathsf{S} & \mathsf{0}_4 \\ \mathsf{0}_4 & \mathsf{I}_4 \end{bmatrix} \qquad \mathsf{S} = \begin{bmatrix} 0 & 0 & -1 \\ 0 & 1 & 0 \\ -1 & 0 & 0 \end{bmatrix}$$

Observe that the permutation matrices for the graphs of order 2 have a 4×4 identity matrix in the last bottom block matrix and so are acting only in $\mathbb{Z}^3 \times 0^4$. The third row of Table 2 represents the equation $E = \kappa_3 \frac{\partial A}{\partial t}\frac{\partial m}{\partial t}$, where A represents an area. The factor $\frac{\partial A}{\partial t}$ represents a diffusion constant D or a flux of vorticity. The fourth row of Table 2 represents the equation $E = \kappa_4 amr$ where a represents the acceleration and where E is recognized as potential energy when $a = g$ with g the acceleration of the Earth gravitation. Both constellations combine to $\kappa_3 \frac{\partial A}{\partial t}\frac{\partial m}{\partial t} = \kappa_4 amr$. We anticipate a first order partial differential equation:

$$\kappa_3 D \frac{\partial m}{\partial t} - \kappa_4 amr = 0 \ .$$

The combinations of the constellations could also generate the following partial differential equation:

$$\kappa_3 \frac{\partial r^2}{\partial t}\frac{\partial m}{\partial t} - \kappa_4 amr = r(2\kappa_3 \frac{\partial r}{\partial t}\frac{\partial m}{\partial t} - \kappa_4 am) = r(2\kappa_3 v \frac{\partial m}{\partial t} - \kappa_4 \frac{\partial v}{\partial t} m) = 0 \ .$$

We see that the form and the combination of constellations is not uniquely defining one equation but a set of equations.

3.3.3. Graphs of order n=8

We analyse the parallelograms in Fig. 1 having frequency $f = n = 8$. The first graph of order 8 corresponds with a parallelogram having the perimeter $p_p = 7,464$ and the second graph of order 8 has a perimeter $p_p = 8,325$. The result for the first and second graphs are given in the Table 3. The components of physical quantities which are *unknown* to the author are marked U_j . The author is not aware if these equations are known to the physics community. Observe that the constellations of graph $g = 1$ are all related to $E(1,2,1) = \kappa_2 \boldsymbol{p} \cdot \boldsymbol{v}$ which is a graph of order $n = 1$.

Table 3: Graphs of order $n = 8$ for *energy*.

n	g	v	p_p	$\breve{x}$	$\breve{y}$	$\breve{x} \cdot \breve{y}$	form
8	1	1	7,464	(1,0,-1,-1,0,0,0)	(1,1,-1,1,0,0,0)	1	$E(8,1,1) = \kappa_1 \frac{v}{I} U_1$
8	1	2	7,464	(1,0,-1,0,-1,0,0)	(1,1,-1,0,1,0,0)	1	$E(8,1,2) = \kappa_2 \frac{v}{T} U_2$
8	1	3	7,464	(1,0,-1,0,0,-1,0)	(1,1,-1,0,0,1,0)	1	$E(8,1,3) = \kappa_3 \frac{v}{n} U_3$
8	1	4	7,464	(1,0,-1,0,0,0,-1)	(1,1,-1,0,0,0,1)	1	$E(8,1,4) = \kappa_4 \frac{v}{L} U_4$
8	1	5	7,464	(1,0,-1,0,0,0,1)	(1,1,-1,0,0,0,-1)	1	$E(8,1,5) = \kappa_5 U_5 \frac{p}{L}$
…	…	…	…	…	…	…	…

n	g	v	p_p	$\breve{x}$	$\breve{y}$	$\breve{x}\cdot\breve{y}$	form
8	1	6	7,464	(1,0,-1,0,0,1,0)	(1,1,-1,0,0,-1,0)	1	$E(8,1,6)=\kappa_6 U_6 \frac{p}{n}$
8	1	7	7,464	(1,0,-1,0,1,0,0)	(1,1,-1,0,-1,0,0)	1	$E(8,1,7)=\kappa_7 U_7 \frac{p}{T}$
8	1	8	7,464	(1,0,-1,1,0,0,0)	(1,1,-1,-1,0,0,0)	1	$E(8,1,8)=\kappa_8 U_8 \frac{p}{I}$
8	2	1	8,325	(0,0,0,-1,0,0,0)	(2,1,-2,1,0,0,0)	-1	$E(8,2,1)=\kappa_9 \frac{1}{I} U_1$
8	2	2	8,325	(0,0,0,0,-1,0,0)	(2,1,-2,0,1,0,0)	-1	$E(8,2,2)=\kappa_{10} \frac{1}{T} U_2$
8	2	3	8,325	(0,0,0,0,0,-1,0)	(2,1,-2,0,0,1,0)	-1	$E(8,2,3)=\kappa_{11} \frac{1}{n} U_3$
8	2	4	8,325	(0,0,0,0,0,0,-1)	(2,1,-2,0,0,0,1)	-1	$E(8,2,4)=\kappa_{12} \frac{1}{L} U_4$
8	2	5	8,325	(0,0,0,0,0,0,1)	(2,1,-2,0,0,0,-1)	-1	$E(8,2,5)=\kappa_{13} L \frac{E}{L}$
8	2	6	8,325	(0,0,0,0,0,1,0)	(2,1,-2,0,0,-1,0)	-1	$E(8,2,6)=\kappa_{14} n \frac{E}{n}$
8	2	7	8,325	(0,0,0,0,1,0,0)	(2,1,-2,0,-1,0,0)	-1	$E(8,2,7)=\kappa_{15} T \frac{E}{T}$
8	2	8	8,325	(0,0,0,1,0,0,0)	(2,1,-2,-1,0,0,0)	-1	$E(8,2,8)=\kappa_{16} I \frac{E}{I}$

The number of signed permutation matrices for graphs of order 8 is $\binom{8}{2}=28$. The permutation matrix $\mathsf{P}_{811,812}$ that transforms the constellation $E(8,1,1)$ in $E(8,1,2)$ is:

$$\mathsf{P}_{811,812}=\begin{bmatrix}1&0&0&0&0&0&0\\0&1&0&0&0&0&0\\0&0&1&0&0&0&0\\0&0&0&0&1&0&0\\0&0&0&0&0&1&0\\0&0&0&0&0&0&1\\0&0&0&1&0&0&0\end{bmatrix}$$

and is one of the 28 permutation matrices describing the connectivity between these 8 constellations. It is obvious that this matrix $\mathsf{P}_{811,812}$ is not symmetric. The permutation matrix $\mathsf{P}_{821,822}$ that transforms the constellation $E(8,2,1)$ in $E(8,2,2)$ is identical to $\mathsf{P}_{811,812}$. Observe that the permutation matrix $\mathsf{P}_{811,812}$ has a block structure:

$$\mathsf{P}_{811,812}=\begin{bmatrix}\mathsf{I}_3&\mathsf{O}_4\\\mathsf{O}_4&\mathsf{T}\end{bmatrix} \qquad \mathsf{T}=\begin{bmatrix}0&1&0&0\\0&0&1&0\\0&0&0&1\\1&0&0&0\end{bmatrix}$$

Observe that the permutation matrices for the graphs of order 8 have a 3×3 identity matrix in the first upper block matrix and so are not transforming the $\mathbb{Z}^3 \times 0^4$. Consider the $\mathbb{Z}$-module $\mathbb{Z}^7$ and the $\mathbb{Z}$-submodule $\mathbb{Z}^3$ then there exist a canonical $\mathbb{Z}$-linear map from $\mathbb{Z}^7$ to the factor group $\mathbb{Z}^7/\mathbb{Z}^3$ that sends a lattice point $\breve{x} \in \mathbb{Z}^7$ to the element $\breve{x} + \mathbb{Z}^3$. We study the dependency of the isoperimeter distribution for the physical quantity *energy* as function of the dimension d of the integer lattice when $3 \leq d \leq 8$. The results (Table 4) show that the frequency f in the isoperimeter distribution for the physical quantity *energy* is *uncorrelated* with the dimension d of the integer lattice when $d \geq 5$ and $f = 1$ or $f = 2$.

Table 4: Variation of the frequency f of the isoperimeter distribution for the physical quantity *energy* as a function of the dimension d of the $\mathbb{Z}$-modules denoted as $\mathbb{Z}^d$ when $3 \leq d \leq 8$.

Id	p_p	$\mathbb{Z}^3$	$\mathbb{Z}^4$	$\mathbb{Z}^5$	$\mathbb{Z}^6$	$\mathbb{Z}^7$	$\mathbb{Z}^8$
1	0	1	1	1	1	1	1
2	6,146	1	1	1	1	1	1
3	6,449	2	2	2	2	2	2
4	6,650	2	2	2	2	2	2
5	6,732	0	2	4	6	8	10
6	6,828	1	1	1	1	1	1
7	7,059	0	4	8	12	16	20
8	7,162	0	2	4	6	8	10
9	7,181	1	5	9	13	17	21
10	7,236	2	2	6	14	26	42
11	7,414	2	4	6	8	10	12
12	7,464	1	1	1	1	1	1

3.4. Case study for the physical quantity force

The lattice point $\breve{z} = (1, 1, -2, 0, 0, 0, 0) = \breve{F}$ represents the physical quantity *force*. The graphical representation (Fig. 3) of the discrete value distribution of parallelogram perimeters p_p for parallelograms representing equations between physical quantities in $\mathbb{Z}^7$ resulting in the physical quantity *force* shows also a rich structure. It reveals the *force* constellations. Observe that the lowest frequency f_{min} in Fig. 3 is $f_{min} = 1$. Detailed analysis of the collinearity of $\breve{x}$ and $\breve{y}$ indicates that the points with perimeter $p_p = 4,899$ and $p_p = 14,697$ are degenerated parallelograms. Observe (Table 5) that the parity of the sum of the coordinates of the lattice points $\breve{x}$ and $\breve{y}$ are always equal. The components of physical quantities which are *unknown* to the author are marked U_j in the equations of components of physical quantities resulting in the physical quantity force.

Table 5: Unique parallelograms in $\mathbb{Z}^7$ for the physical quantity *force*.

p_p	$\breve{x}$	$\breve{y}$	$\breve{x} \cdot \breve{y}$	form
4,899	(1,1,-2,0,0,0,0)	(0,0,0,0,0,0,0)	0	$\boldsymbol{F} = \kappa_1 \boldsymbol{F}_0$
5,464	(1,1,-1,0,0,0,0)	(0,0,-1,0,0,0,0)	1	$\boldsymbol{F} = \kappa_2 \frac{\boldsymbol{dp}}{dt}$
5,657	(1,0,-1,0,0,0,0)	(0,1,-1,0,0,0,0)	1	$\boldsymbol{F} = \kappa_3 \boldsymbol{v} \frac{\partial m}{\partial t}$
...	...	...	...	...

p_p	$\breve{x}$	$\breve{y}$	$\breve{x}\cdot\breve{y}$	form
8,633	(0,0,1,0,0,0,0)	(1,1,-3,0,0,0,0)	-3	$\boldsymbol{F}=\kappa_4 t\frac{\boldsymbol{dF}}{dt}$
11,710	(-1,-1,1,0,0,0,0)	(2,2,-3,0,0,0,0)	-7	$\boldsymbol{F}=\kappa_5 U_1\frac{dp^2}{dt}$
14,697	(-1,-1,2,0,0,0,0)	(2,2,-4,0,0,0,0)	-12	$\boldsymbol{F}=\kappa_6 U_2 F^2$
18,122	(-1,-1,3,0,0,0,0)	(2,2,-5,0,0,0,0)	-19	$\boldsymbol{F}=\kappa_7 U_3\frac{dF^2}{dt}$
21,361	(-2,-2,3,0,0,0,0)	(3,3,-5,0,0,0,0)	-27	$\boldsymbol{F}=\kappa_8\frac{1}{(\frac{dp^2}{dt})}(\frac{dp}{dt})^2\boldsymbol{p}$

Wilczek [42, 43, 44] elaborated on Newton's second law $\boldsymbol{F}=m\boldsymbol{a}$. We observe that this form of constellation is not appearing in the list of unique parallelograms. We don't find the lattice points (0,1,0,0,0,0,0) and (1,0,-2,0,0,0,0) as vertices of *unique* parallelograms, which is in correspondence with Wilczek's arguments. What we observe in the detailed data of the discrete value distribution is the occurrence of $\boldsymbol{F}=m\boldsymbol{a}$ in a constellation with the form $\kappa_8\boldsymbol{r}\frac{\partial^2 m}{\partial t^2}=\kappa_9 m\boldsymbol{a}$, having frequency $f=2$ for a perimeter $p_p=6,472$. The second row is the basic form where the force is expressed as the time derivative of the linear momentum [42]. The relation between *force* and *energy*, where a force is expressed as the space derivative of the energy [42] is found in the discrete value distribution at perimeter $p_p=8$ and has frequency $f=26$. At perimeter $p_p=10,312$ we find another constellation form $\kappa_{10}\frac{\partial E}{\partial t}\frac{\partial m}{\partial t}=\kappa_{11}vU_4$ with frequency $f=2$. The list (Table 5) of vertices, as well as the complete distribution is derived purely mathematically without *a priori* knowledge of physics using an algorithm Appendix A based on discrete geometry. Observe in Fig. 4 that all the unique *force* constellations are embedded in $\mathbb{Z}^3\times 0^4$ and localized in the hyperplane $H_{\breve{b}}=\{(X^1,\dots,X^7)\mid X^1-X^2=0\}$ with $\breve{b}=(1,-1,0,0,0,0,0)$ that represents the reciprocal of the *linear density*. One exception is observed for the equation $\boldsymbol{F}=\kappa_2\boldsymbol{v}\frac{\partial m}{\partial t}$ that forms a parallelogram orthogonal to the hyperplane $H_{\breve{b}}$. Observe in Fig. 4 the symmetry axes determined by the line containing *origin* and *force* and the line containing the *time derivative* and *impulse*.

3.5. Invariance of the isoperimetric distribution

Theorem 1. *The isoperimetric distribution, for parallelograms containing the integer lattice points $\breve{o}$ and $\breve{z}$, is invariant when the coordinates of the integer lattice point $\breve{z}$ are subjected to a signed permutation.*

Proof. The isometric property of the above mapping and mapping combinations is the origin of the invariance in the isoperimetric distribution [45]. The perimeter of the parallelogram is based on the Euclidean distance (ℓ_2-distance) between the lattice points and so neither a permutation of the coordinates nor a change in the sign of the coordinates will modify the value of the distance between the lattice points. □

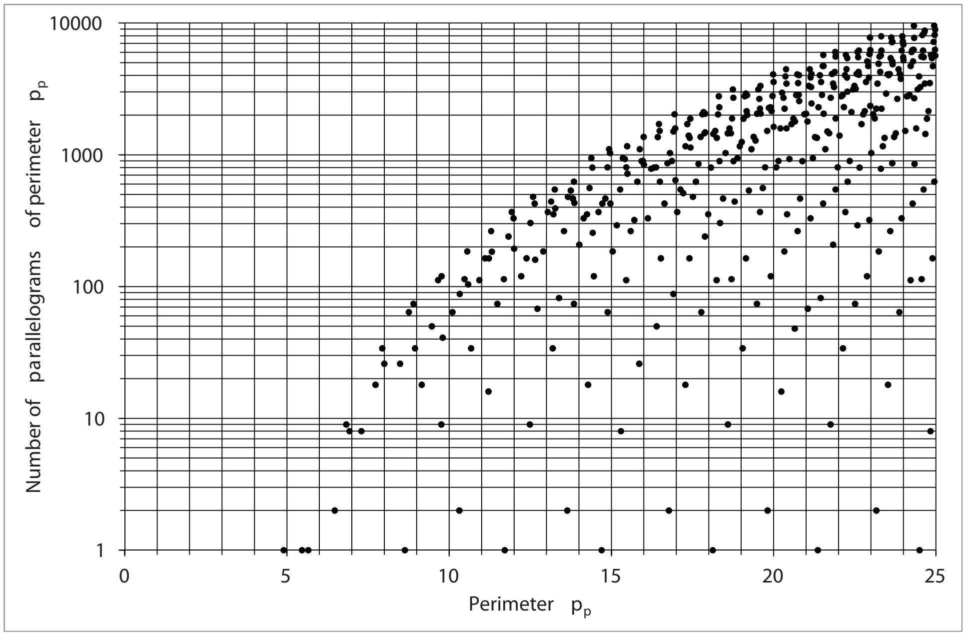

Figure 3: Discrete value distribution of parallelogram perimeters p_p in $\mathbb{Z}^7$ resulting in the physical quantity *force*.

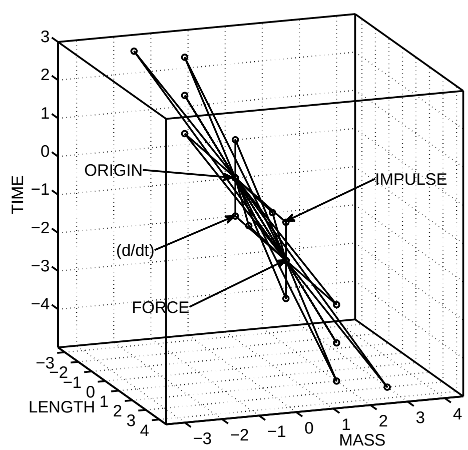

Figure 4: Unique parallelograms resulting in the physical quantity *force*.

For n-ary equations where $n \geq 4$ we have not a parallelogram, however the isometry properties remain valid when considering the path length of the path connecting the $n+1$ lattice points of the constellation. The automorphism group of the 7-dimensional cubic lattice $\mathrm{Aut}(\mathbb{Z}^7)$ contains all permutations and sign changes of the 7 coordinates and has order $2^7\, 7! = 645120$. Each signed permutation matrix is an orthogonal matrix [45].

Example 3.3. The components of the physical quantity *force*, represented by (1, 1, -2, 0, 0, 0, 0), and the components of the physical quantity *angular momentum*, represented by (2, 1, -1, 0, 0, 0, 0), have the same isoperimetric distribution.

Example 3.4. The components of the physical quantity *mass*, represented by (0, 1, 0, 0, 0, 0, 0), and the components of the physical quantity *frequency*, represented by (0, 0, -1, 0, 0, 0, 0), have the same isoperimetric distribution.

The fact that some physical quantities are related through a signed permutation implies that these physical quantities are *qualitatively* indistinguishable [46]. Feynman remarks that *"the fundamental laws of physics, when discovered, can appear in so many different forms that are not apparently identical at first, but with a little mathematical fiddling you can show the relationship"* [7]. These many different forms are what we define as the *constellations* of the physical quantity and the graphs of order n express the relationship between these geometrical forms.

4. Classification of components of physical quantities

To classify the components of physical quantities we need to find a partitioning of the integer lattice $\mathbb{Z}^7$. It is known from linear vector quantization [47, 48, 49] that the ℓ_2-norm and the phase of a lattice point are used to partition a lattice. However, this norm and phase are not the correct classifiers for the physical quantities. If we use as classifier the ℓ_∞-norm we obtain equivalence classes for which the elements of the class have the *same* isoperimetric distribution.

4.1. Measure polytope properties

Theorem 2. *Let P_d^s be a centrally symmetric d-dimensional measure polytope of edge-length 2s then the cardinality of P_d^s is $(2s+1)^d$.*

Proof. For $d = 0$ the result is trivial.
For $d = 1$ we have the set $P_1^s = \{-s, \ldots, 0, \ldots, s\}$ with edge-length $2s$. Let us denote the cardinality of the set S by $\#(S)$ then $\#(P_1^s) = 2s + 1$.
For $d = 2$ we have to increase the dimension d by 1, which corresponds to calculate the Cartesian product of the sets $P_1^s \times P_1^s = P_2^s$.
It is a property of cardinal numbers [50] that: $\#(P_2^s) = \#(P_1^s) \times \#(P_1^s) = \#(P_1^s) \cdot \#(P_1^s) = (2s+1)^2$. Assume that $\#\left(P_{d-1}^s\right) = (2s+1)^{d-1}$. Then $\#(P_d^s) = \#\left(P_{d-1}^s\right) \cdot \#(P_1^s) = (2s+1)^{d-1} \cdot (2s+1) = (2s+1)^d$. □

We distinguish the measure polytope P_d^s by the parameters d and s, where d represents the dimension of the integer lattice and s represents the edge length. We define a leader class of a measure polytope as:

Definition 2. A leader class of a measure polytope is the set of lattice points of $\mathbb{Z}^7$ that have the same isoperimetric distribution.

A leader class of a measure polytope of $\mathbb{Z}^7$ is noted as $[(X^1, \ldots, X^7)]$ where $(X^1, \ldots, X^7)$ are the coordinates of the representative lattice point. Each leader class forms a set of lattice points that are symmetric about the origin. The cardinality of a leader class of a measure polytope is calculated using elementary combinatorics. Let $A = \{0, 1, 2, \ldots, k\}$ be the alphabet of measure polytope with edge length $2k$. The representative of a leader class of a measure polytope is a word w constructed from the alphabet A. The words w have a length d that corresponds to the dimension of $\mathbb{Z}^7$. Let d_i be the number of characters of type i of the alphabet A. Suppose that the characters are subjected to permutation and change of sign, then using combinatorics the cardinality is given by the equation

$$\#\,(w) = 2^{d-d_0} \frac{d!}{d_0! d_1! d_2! \ldots d_k!} \,. \tag{2}$$

Observe that each measure polytope in $\mathbb{Z}^7$ represents a centrally symmetric lattice polytope [27, 51, 52, 53]. The number of vertices in each leader class is equal to the cardinality of w. Observe also that the representative lattice point, in coding theory [47] called an *absolute leader*, has only coordinates that are *non-negative integers*. We define the total degree of a monomial as:

Definition 3. A monomial m in $u_1, u_2, \ldots, u_7$ is a product of the form:

$$m = \prod_{i=1}^{7} u_i^{X^i} \,, \tag{3}$$

where all the exponents $X^i \in \mathbb{Z}_+$ and $u_i \in \mathcal{U}$ (see section 1). The total degree deg of this monomial is the sum $X^1 + \ldots + X^7$.

From the 7-tuple of non-negative integer exponents $(X^1, \ldots, X^7) \in \mathbb{Z}_+^7$ a monomial [54] is constructed one-to-one of the form $m = \prod_{i=1}^{7} u_i^{X^i}$ that we compare with equation (**??**). It means that a lot of results known from the commutative module of monomials are applicable to the classification of the components of physical quantities. The number of classes of monomials (Table 6) with Chebyshev norm $\|\breve{x}\|_\infty \leq s$ in $\mathbb{Z}^7$ is the result from application of lemma 4 [55].

Table 6: Properties of the measure polytopes P_7^s in $\mathbb{Z}^7$ for $s \leq 10$.

$\|\breve{x}\|_\infty = s$	sum($\#\,([a])$)	cumul(sum($\#\,([a])$))	$\#\,(P_7^s)$	cumul($\#\,(P_7^s)$)
0	1	1	1	1
1	2186	2187	7	8
2	75938	78125	28	36
3	745418	823543	84	120
4	3959426	4782969	210	330
5	14704202	19487171	462	792
6	43261346	62748517	924	1716
7	108110858	170859375	1716	3432
8	239479298	410338673	3003	6435
9	483533066	893871739	5005	11440
10	907216802	1801088541	8008	19448

In (Table 6) the second column shows the number of vertices while the third column gives the cumulated number of vertices. The fourth and fifth columns have a similar meaning but are expressing the number of classes in each measure polytope P_7^s .

4.2. Enumeration of the measure polytopes

The enumeration table (Table C.9) of the measure polytope P_7^3 consists of 8 columns. The second column is the row identifier. The third column gives the representative of the leader class. The fourth column contains the sum of the absolute value of the coordinates of the lattice points being elements of the leader class that is exclusively the total degree of the monomial associated with the leader class. The fifth column gives the parity of the representative of the leader class. The sixth column gives the ℓ_1-norm of the representative. The seventh column gives the cardinality of the leader class. The eighth column gives the Gödel number of the representative. The ordering of the classes is based on *graded reverse lex order* [54]. We derive from Table 6 that the measure polytopes P_7^s are partitioned in $\binom{7+s-1}{s}$ equivalence classes. The cardinality of the leader classes is related to the theta series of the integer lattice $\mathbb{Z}^7$. We find in the OEIS [40] the sequence A008451 given by $r_7(N) =$ 1, 14, 84, 280, 574, 840, 1288, 2368, 3444, 3542, 4424, 7560, 9240, 8456, 11088, 16576, 18494, 17808, 19740, 27720, 34440, 29456, 31304, 49728, 52808, 43414, 52248, 68320, 74048, 68376, 71120, 99456, 110964, 89936, 94864, 136080 . . . . The sequence represents the number of ways of writing a positive integer N as a sum of *seven* integral squares and is defined by:

$$\Theta_{\mathbb{Z}^7}(z) = \sum_{N=0}^{\infty} r_7(N) q^N \ , \tag{4}$$

where $q = e^{\pi i z}$ and N is the norm of the lattice point [56]. The enumeration table (Table D.10) gives the relation between the sequence A008451 and the partitioning of 7-spheres in leader classes of the measure polytopes. The common physical quantities (Table **??**) which belong to the measure polytopes, where the variable $\|\breve{x}\|_\infty = s$ taking values from 0 to 10, are enumerated. Table **??** is far from exhaustive, but it highlights the sparse distribution of the common physical quantities when taking in consideration the cardinalities (Table 6) of classes and vertices.

5. Paths, walks and cycles in a 7-dimensional integer lattice

A path in $\mathbb{Z}^7$ is a non-empty graph $P = (V, E)$ of the form $V = \{\breve{x}_0, \dots, \breve{x}_k\}$ and $E = \{\breve{x}_0\breve{x}_1, \dots, \breve{x}_{k-1}\breve{x}_k\}$ where the $\breve{x}_i$ are all distinct [33]. As we will connect points in the integer lattice forming parallelograms, we use the term *k-cycle* from graph theory [33], where the k-cycle is a simple graph of length k, i.e., consisting of k vertices and k edges and represented by a sequence of consecutive vertices $\breve{x}_0 \dots \breve{x}_{k-1}\breve{x}_0$. Equations between physical quantities are represented by paths in $\mathbb{Z}^7$. Dimensional products are represented by cycles in $\mathbb{Z}^7$. A *walk of length k* in $\mathbb{Z}^7$ is a non-empty alternating sequence $\breve{v}_0 e_0 \breve{v}_1 e_1 \dots e_{k-1} \breve{v}_k$ of vertices $\breve{v}_i$ and edges e_i in $\mathbb{Z}^7$ such that $e_i = \{\breve{v}_i, \breve{v}_{i+1}\}$ for all $i < k$.

5.1. Gödel walk in a 7-dimensional integer lattice

We encode each integer lattice point of $\mathbb{Z}^7_+$ by using a similar scheme to the Gödel encoding [57] applied to 7 non-negative integer variables. We define the *Gödel number* in $\mathbb{Z}^d_+$, where d is the dimension of the integer lattice:

$$\phi_d(X^1 \dots X^d) = \prod_{i=1}^{d} p_i^{X^i} \ , \tag{5}$$

where p_i is the i-th prime number, $\breve{x} = (X^1, \ldots, X^d)$ and $X^i \in \mathbb{Z}_+$.

Example 5.1. $\phi_7(1110000) = 2^1 \cdot 3^1 \cdot 5^1 \cdot 7^0 \cdot 11^0 \cdot 13^0 \cdot 17^0 = 30$

This encoding which we denote as ϕ_7 is injective between $\mathbb{Z}_+^7$ and $\mathbb{Z}_+$. The range of ϕ_7 is a subset Φ_7 of the non-negative integers $\mathbb{Z}_+$ because all the primes which are different from the first 7 primes are not images of lattice points of $\mathbb{Z}_+^7$, as well as all the composite numbers having divisors larger than 17. Observe that each of the base physical quantities of the set $\mathcal{B}$ are assigned to a prime number. The base physical quantities play the same role as the prime numbers, being the *atoms* in number theory [58]. If we walk through the integer sublattice $\mathbb{Z}_+^7$ respecting the ordering created by the Gödel encoding, then we generate a series of segments in $\mathbb{Z}_+^7$. We call this walk a *Gödel walk* through the integer sublattice $\mathbb{Z}_+^7$. The segments are known in number theory as the prime gaps $g(p) = n$ of gap length n. All the leader class representatives are located on the Gödel walk. When the Gödel walk is performed in $\mathbb{Z}_+^{25}$ then all the first 100 non-negative integers will be visited (Fig. 5). When restricting the dimension to $d = 7$ we find 67 non-negative integers that will be visited. An enumeration (Table **??**) of the first 67 lattice points shows also the crossings of the Gödel walk with the measure polytopes P_7^s . The *successive* lattice points of the Gödel walk are *orthogonal* when calculated for the first 100 lattice points in the integer lattice $\mathbb{Z}_+^{25}$. Observe that the Gödel walk represents a unique walk in $\mathbb{Z}_+^k$, where $k \in \mathbb{Z}_+$ because it requires orthogonality between successive lattice points and because it *minimizes* the function ϕ_k at each lattice point. There are 23 segments in $\mathbb{Z}_+^7$ and 28 segments in $\mathbb{Z}_+^3$ for the first 100 non-negative integers. The orthogonality between successive lattice points remains valid within the segments that have more than 1 lattice point. This walk encodes all the physical quantities of $\mathbb{Z}_+^7$ up to a signed permutation. Observe that the leader class representative has always the *smallest* Gödel number of the class. Physicists represent *correlations* between physical quantities graphically in the form of *cubes* that contain the respective physical quantities as the axes of the cube. The Gödel walk presents a *natural* way of selecting mutually orthogonal sequential physical quantities. Inspection of the list (Table **??**) results in cubes $C(i, j, k)$, where i, j, k are successive Gödel numbers. We find 7 cubes $C(3, 4, 5) = \{M, L^2, T\}$, $C(5, 6, 7) = \{T, ML, I\}$, $C(7, 8, 9) = \{I, L^3, M^2\}$, $C(9, 10, 11) = \{M^2, LT, \Theta\}$, $C(11, 12, 13) = \{\Theta, ML^2, N\}$, $C(13, 14, 15) = \{N, LI, MT\}$, $C(15, 16, 17) = \{MT, L^4, J\}$ where we use the agreed [28] symbol for the dimensions.

Example 5.2. The quantity ML in the cube $C(5, 6, 7) = \{T, ML, I\}$ could be expressed as function of $\frac{\hbar}{c}$ and the product $T \times I$ is nothing else than the electric charge. The Compton effect for an electron can be represented by a volume $\frac{e\hbar}{c}$ in the cube $C(5, 6, 7)$.

The mutual orthogonality in the 7 cubes is *invariant* when the integer lattice points representing the cube axes are subject to a signed permutation. We transform the set $\{M, L^2, T\}$ in $\{M, L^2, T^{-1}\}$ and observe that the volume of the new cube represents the *angular momentum.* The set $\{M^2, LT, \Theta\}$ can be transformed to $\{M^2, LT^{-1}, \Theta\}$ representing a cube with on the x-axis the *mass squared*, on the y-axis the *speed* and on the z-axis the *thermodynamic temperature.*

5.2. Additive partitioning of leader classes

The encoding of the leader classes with a Gödel number allows the factorization of the Gödel number in distinct factors. Richard J. Mathar (http://home.strw.leidenuniv.nl/ mathar/) has listed in the OEIS [40] the integer series A045778 that gives the factorization of non-negative integers up

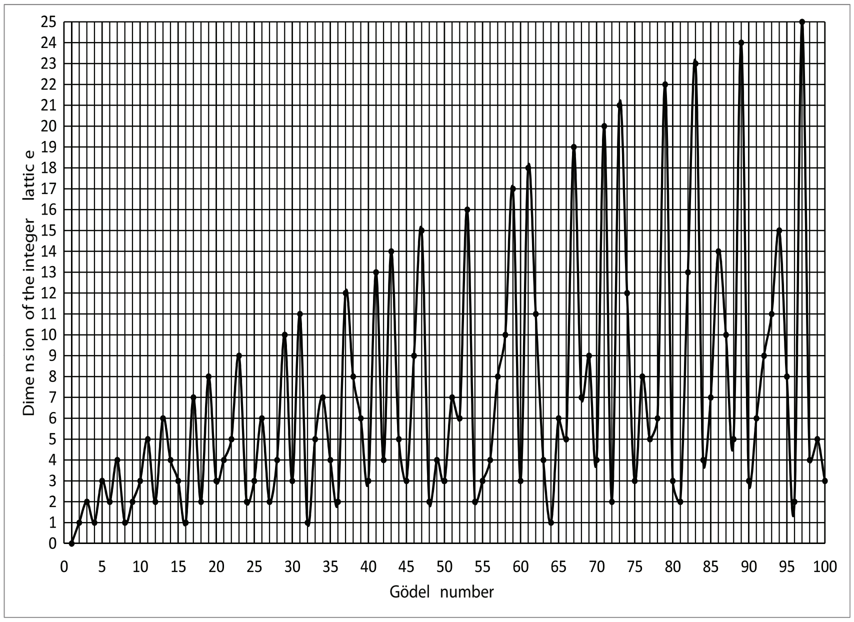

Figure 5: Gödel walk in $\mathbb{Z}_+^{25}$.

to n=1500. In the present article we focussed on the most elementary constellation of lattice points that form a parallelogram. The leader class is the representative for all the physical quantities which are vertices of a partition of a measure polytope P_7^s . A signed permutation can be found that maps the factored equations to equivalent equations of the desired physical quantity that is an element of the leader class. We show the method for the physical quantity *energy*.

Example 5.3. The leader class for *energy* is $[2^2 10^4]$. It has Gödel number $\phi_7(2210000) = 180$. From the OEIS[40] A045778 series we find as factorizations:

$$180 = 2 \times 3 \times 5 \times 6$$

The 4-factoring results in 1 equation that represents a 5-ary equation. By applying the Gödel decoding on the 4-factoring of $\phi_7(2210000) = 180$, we find the additive partitioning of the leader class representative $(2, 2, 1, 0, 0, 0, 0)$ in a 5-ary equation:

(i) $(2, 2, 1, 0, 0, 0, 0) = (0, 0, 0, 0, 0, 0, 0) + (1, 0, 0, 0, 0, 0, 0) + (0, 1, 0, 0, 0, 0, 0) + (0, 0, 1, 0, 0, 0, 0) + (1, 1, 0, 0, 0, 0, 0)$;

$180 = 2\times3\times30 = 2\times5\times18 = 2\times6\times15 = 2\times9\times10 = 3\times4\times15 = 3\times5\times12 = 3\times6\times10 = 4\times5\times9$

The 3-factoring results in 8 equations that represent each a 4-ary equation. The additive partitioning of the leader class representative (2,2,1,0,0,0,0) in 4-ary equations are:

(i) $(2, 2, 1, 0, 0, 0, 0) = (0, 0, 0, 0, 0, 0, 0) + (1, 0, 0, 0, 0, 0, 0) + (0, 1, 0, 0, 0, 0, 0) + (1, 1, 1, 0, 0, 0, 0)$

(ii) $(2, 2, 1, 0, 0, 0, 0) = (0, 0, 0, 0, 0, 0, 0) + (1, 0, 0, 0, 0, 0, 0) + (0, 0, 1, 0, 0, 0, 0) + (1, 2, 0, 0, 0, 0, 0)$

(iii) $(2,2,1,0,0,0,0) = (0,0,0,0,0,0,0) + (1,0,0,0,0,0,0) + (1,1,0,0,0,0,0) + (0,1,1,0,0,0,0)$

(iv) $(2,2,1,0,0,0,0) = (0,0,0,0,0,0,0) + (1,0,0,0,0,0,0) + (0,2,0,0,0,0,0) + (1,0,1,0,0,0,0)$

(v) $(2,2,1,0,0,0,0) = (0,0,0,0,0,0,0) + (0,1,0,0,0,0,0) + (2,0,0,0,0,0,0) + (0,1,1,0,0,0,0)$

(vi) $(2,2,1,0,0,0,0) = (0,0,0,0,0,0,0) + (0,1,0,0,0,0,0) + (0,0,1,0,0,0,0) + (2,1,0,0,0,0,0)$

(vii) $(2,2,1,0,0,0,0) = (0,0,0,0,0,0,0) + (0,1,0,0,0,0,0) + (1,1,0,0,0,0,0) + (1,0,1,0,0,0,0)$

(viii) $(2,2,1,0,0,0,0) = (0,0,0,0,0,0,0) + (2,0,0,0,0,0,0) + (0,0,1,0,0,0,0) + (0,2,0,0,0,0,0)$

$$180 = 2 \times 90 = 3 \times 60 = 4 \times 45 = 5 \times 36 = 6 \times 30 = 9 \times 20 = 10 \times 18 = 12 \times 15$$

The 2-factoring results also in 8 equations that represent each a ternary equation. The additive partitioning of the leader class representative $(2,2,1,0,0,0,0)$ in 3-ary equations are:

(i) $(2,2,1,0,0,0,0) = (0,0,0,0,0,0,0) + (1,0,0,0,0,0,0) + (1,2,1,0,0,0,0)$

(ii) $(2,2,1,0,0,0,0) = (0,0,0,0,0,0,0) + (0,1,0,0,0,0,0) + (2,1,1,0,0,0,0)$

(iii) $(2,2,1,0,0,0,0) = (0,0,0,0,0,0,0) + (2,0,0,0,0,0,0) + (0,2,1,0,0,0,0)$

(iv) $(2,2,1,0,0,0,0) = (0,0,0,0,0,0,0) + (0,0,1,0,0,0,0) + (2,2,0,0,0,0,0)$

(v) $(2,2,1,0,0,0,0) = (0,0,0,0,0,0,0) + (1,1,0,0,0,0,0) + (1,1,1,0,0,0,0)$

(vi) $(2,2,1,0,0,0,0) = (0,0,0,0,0,0,0) + (0,2,0,0,0,0,0) + (2,0,1,0,0,0,0)$

(vii) $(2,2,1,0,0,0,0) = (0,0,0,0,0,0,0) + (1,0,1,0,0,0,0) + (1,2,0,0,0,0,0)$

(viii) $(2,2,1,0,0,0,0) = (0,0,0,0,0,0,0) + (2,1,0,0,0,0,0) + (0,1,1,0,0,0,0)$

We conclude that the leader class representative $(2,2,1,0,0,0,0)$ can be partitioned in 17 distinct terms. As this leader class is representative for the physical quantity energy we conclude to the existence of *17 distinct forms* of equations representing the physical quantity energy. Generalisation of this methodology will reveal the generic constellations for the leader class representatives.
The signed permutation matrix $\mathsf{P}_{\mathsf{energy}}$ transforms the leader class representative $(2,2,1,0,0,0,0)$ in the lattice point $(2,1,-2,0,0,0,0)$ and is given below:

$$\mathsf{P}_{\mathsf{energy}} = \begin{bmatrix} 1 & 0 & 0 & 0 & 0 & 0 & 0 \\ 0 & 0 & 1 & 0 & 0 & 0 & 0 \\ 0 & -1 & 0 & 0 & 0 & 0 & 0 \\ 0 & 0 & 0 & 1 & 0 & 0 & 0 \\ 0 & 0 & 0 & 0 & 1 & 0 & 0 \\ 0 & 0 & 0 & 0 & 0 & 1 & 0 \\ 0 & 0 & 0 & 0 & 0 & 0 & 1 \end{bmatrix} \tag{7}$$

We apply the matrix $\mathsf{P}_{\mathsf{energy}}$ on the seventeen equations that represent the additive partitions of the leader class representative (2,2,1,0,0,0,0) and find the *energy* equations given in Table 7 . The columns marked $\breve{i}$, $\breve{j}$, $\breve{k}$, $\breve{l}$ and $\breve{m}$ contain the 17 lattice points in $\mathbb{Z}^7$ forming the *energy* constellation.

Table 7: Complete set of generic equations for the quantity *energy*.

$\breve{i}$	$\breve{j}$	$\breve{k}$	$\breve{l}$	$\breve{m}$	form
(0^7)	$(1,0^6)$	$(0,0,-1,0^4)$	$(0,1,0^5)$	$(1,0,-1,0^4)$	$E_1 = \kappa_1 x\nu m v$
(0^7)	$(1,0^6)$	$(0,0,-1,0^4)$	$(1,1,-1,0^4)$	(0^7)	$E_2 = \kappa_2 x\nu p$
(0^7)	$(1,0^6)$	$(0,1,0^5)$	$(1,0,-2,0^4)$	(0^7)	$E_3 = \kappa_3 x m a$
(0^7)	$(1,0^6)$	$(1,0,-1,0^4)$	$(0,1,-1,0^4)$	(0^7)	$E_4 = \kappa_4 x v \dfrac{\partial m}{\partial t}$
(0^7)	$(1,0^6)$	$(0,0,-2,0^4)$	$(1,1,0^5)$	(0^7)	$E_5 = \kappa_5 x\nu^2 \int m dx$
(0^7)	$(0,0,-1,0^4)$	$(2,0^6)$	$(0,1,-1,0^4)$	(0^7)	$E_6 = \kappa_6 \nu x^2 \dfrac{\partial m}{\partial t}$
(0^7)	$(0,0,-1,0^4)$	$(0,1,0^5)$	$(2,0,-1,0^4)$	(0^7)	$E_7 = \kappa_7 \nu m \dfrac{\partial A}{\partial t}$
(0^7)	$(0,0,-1,0^4)$	$(1,0,-1,0^4)$	$(1,1,0^5)$	(0^7)	$E_8 = \kappa_8 \nu v \int m dx$
(0^7)	$(2,0^6)$	$(0,1,0^5)$	$(0,0,-2,0^4)$	(0^7)	$E_9 = \kappa_9 x^2 m \nu^2$
(0^7)	$(1,0^6)$	$(1,1,-2,0^4)$	(0^7)	(0^7)	$E_{10} = \kappa_{10} x F$
(0^7)	$(0,0,-1,0^4)$	$(2,1,-1,0^4)$	(0^7)	(0^7)	$E_{11} = \kappa_{11} \nu J$
(0^7)	$(2,0^6)$	$(0,1,-2,0^4)$	(0^7)	(0^7)	$E_{12} = \kappa_{12} x^2 \dfrac{\partial^2 m}{\partial t^2}$
(0^7)	$(0,1,0^5)$	$(2,0,-2,0^4)$	(0^7)	(0^7)	$E_{13} = \kappa_{13} m v^2$
(0^7)	$(1,0,-1,0^4)$	$(1,1,-1,0^4)$	(0^7)	(0^7)	$E_{14} = \kappa_{14} v p$
(0^7)	$(0,0,-2,0^4)$	$(2,1,0^5)$	(0^7)	(0^7)	$E_{15} = \kappa_{15} \nu^2 \int\int m dA$
(0^7)	$(1,1,0^5)$	$(1,0,-2,0^4)$	(0^7)	(0^7)	$E_{16} = \kappa_{16} a \int m dx$
(0^7)	$(2,0,-1,0^4)$	$(0,1,-1,0^4)$	(0^7)	(0^7)	$E_{17} = \kappa_{17} \dfrac{\partial A}{\partial t} \dfrac{\partial m}{\partial t}$

The symbols used in the column *form* have the following interpretation: E_i: energy; x: position, distance; t: time; ν: frequency; m: mass; A: area; v: speed; F: force; J: angular momentum; p: linear momentum; a: acceleration; κ_i: dimensionless variable. The same methodology, as shown for the physical quantity energy, can be applied to any physical quantity. This will then generate for that physical quantity its complete set of generic equations. Table **??** enumerates for leader classes with Gödel number ≤ 1500 the factorization of the Gödel number in i distinct factors. The number of distinct factors is found in the repective columns Fi where $i \in [2, \ldots, 5]$. We conclude that there is a finite number of distinct equations for each physical quantity.

5.3. Bicolouring of a 4-cycle representing an equation between physical quantities

The hypothesis of the existence of *rules* that have to be respected by the *laws of physics*, has been proposed by Wigner and Feynman, see Lange[10]. We elaborate on this problem by proving *one* of these rules applicable for ternary equations $[z] = [\kappa][x][y]$ between the distinct physical quantities $[\kappa], [x], [y], [z]$. The rule constraints the bicolouring of 4-cycles [59, 60, 61] in $\mathbb{Z}^7$.

Theorem 3. *Any ternary equation* $[z] = [\kappa][x][y]$ *between distinct physical quantities* $[\kappa], [x], [y], [z]$ *represents a distinct colouring pattern* $(\operatorname{psc}(\breve{o}), \operatorname{psc}(\breve{x}), \operatorname{psc}(\breve{y}), \operatorname{psc}(\breve{z}))$ *that is an element of the set of colouring patterns* $\{(0,0,0,0), (0,0,1,1), (0,1,0,1), (0,1,1,0)\}$.

Proof. We will use the method *proof by exhaustion* for this theorem. Let the four distinct integer lattice points $\breve{o}, \breve{y}, \breve{z}, \breve{y}$ be the vertices of a *parallelogram*, represented by the 4-cycle $\breve{o}\breve{y}\breve{z}\breve{x}\breve{o}$. The parallelogram is the representation of the ternary equation $[z] = [\kappa][x][y]$ in the integer lattice $\mathbb{Z}^7$. Let the colouring pattern be defined by the 4-tuple $(\operatorname{psc}(\breve{o}), \operatorname{psc}(\breve{x}), \operatorname{psc}(\breve{y}), \operatorname{psc}(\breve{z}))$ in which $\breve{o}$ is the origin of $\mathbb{Z}^7$. By convention $\operatorname{psc}(\breve{o})$ is placed as the first element and $\operatorname{psc}(\breve{z})$ as the last element in the colouring patterns. By the definition of the "psc" function we obtain $\operatorname{psc}(\breve{o}) = 0$. A 4-tuple having only two characters {0,1} has in total $2^4 = 16$ combinations of 4-tuples. So, we will review the 16 cases. The condition that the first element of the 4-tuple has to be 0 reduces the number of combinations to $2^3 = 8$ being the set of colouring patterns {(0,0,0,0), (0,0,0,1), (0,0,1,0), (0,0,1,1), (0,1,0,0), (0,1,0,1),(0,1,1,0), (0,1,1,1)}. The four distinct integer lattice points $\breve{o}, \breve{x}, \breve{y}, \breve{z}$ of the parallelogram have the property $\breve{x} + \breve{y} = \breve{z}$, see Fig. **??**. From elementary number theory [62], it is known that:

$$\text{(i)}\quad \text{even} \pm \text{even} = \text{even}$$

$$\text{(ii)}\quad \text{odd} \pm \text{odd} = \text{even}$$

$$\text{(iii)}\quad \text{even} \pm \text{odd} = \text{odd}$$

The function "psc" is binary-valued on $\mathbb{Z}^7$ satisfying $\operatorname{psc}(\breve{x} + \breve{y}) = \operatorname{psc}(\breve{x}) + \operatorname{psc}(\breve{y})$ for all $\breve{x}, \breve{y} \in \mathbb{Z}^7$. Thus the 4-tuples have the form $(0, \operatorname{psc}(\breve{x}), \operatorname{psc}(\breve{y}), \operatorname{psc}(\breve{x}) + \operatorname{psc}(\breve{y}))$ resulting in the following cases:

Case 1. (0,0,0,0)
If $\operatorname{psc}(\breve{x}) = \operatorname{psc}(\breve{y}) = 0$ then by number theory $\operatorname{psc}(\breve{x}) + \operatorname{psc}(\breve{y}) = 0$. The colouring pattern **(0,0,0,0)** satisfies the above property and is a *valid* colouring pattern. This colouring pattern is called monochromatic.

Case 2. (0,0,0,1)
If $\operatorname{psc}(\breve{x}) = \operatorname{psc}(\breve{y}) = 0$ then by number theory $\operatorname{psc}(\breve{x}) + \operatorname{psc}(\breve{y}) = 0$. The colouring pattern (0,0,0,1) violates the above property and is a *forbidden* colouring pattern.

Case 3. (0,0,1,0)
If $\operatorname{psc}(\breve{x}) = 0$ and $\operatorname{psc}(\breve{y}) = 1$ then by number theory $\operatorname{psc}(\breve{x}) + \operatorname{psc}(\breve{y}) = 1$. The colouring pattern (0,0,1,0) violates the above property and is a *forbidden* colouring pattern.

Case 4. (0,0,1,1)
If $\operatorname{psc}(\breve{x}) = 0$ and $\operatorname{psc}(\breve{y}) = 1$ then by number theory $\operatorname{psc}(\breve{x}) + \operatorname{psc}(\breve{y}) = 1$. The colouring pattern **(0,0,1,1)** satisfies the above property and is a *valid* colouring pattern. This colouring pattern is called two-coloured of pattern 2+2.

Case 5. (0,1,0,0)
If $\text{psc}(\breve{x}) = 1$ and $\text{psc}(\breve{y}) = 0$ then by number theory $\text{psc}(\breve{x}) + \text{psc}(\breve{y}) = 1$. The colouring pattern (0,1,0,0) violates the above property and is a *forbidden* colouring pattern.

Case 6. (0,1,0,1)
If $\text{psc}(\breve{x}) = 1$ and $\text{psc}(\breve{y}) = 0$ then by number theory $\text{psc}(\breve{x}) + \text{psc}(\breve{y}) = 1$. The colouring pattern **(0,1,0,1)** satisfies the above property and is a *valid* colouring pattern. This colouring pattern is called mixed two-coloured.

Case 7. (0,1,1,0)
If $\text{psc}(\breve{x}) = 1$ and $\text{psc}(\breve{y}) = 1$ then by number theory $\text{psc}(\breve{x}) + \text{psc}(\breve{y}) = 0$. The colouring pattern **(0,1,1,0)** satisfies the above property and is a *valid* colouring pattern. This colouring pattern is called two-coloured of pattern 1+2+1.

Case 8. (0,1,1,1)
If $\text{psc}(\breve{x}) = 1$ and $\text{psc}(\breve{y}) = 1$ then by number theory $\text{psc}(\breve{x}) + \text{psc}(\breve{y}) = 0$. The colouring pattern (0,1,1,1) violates the above property and is a *forbidden* colouring pattern.

We obtain as *valid* colouring patterns: $(0,0,0,0)$, $(0,0,1,1)$, $(0,1,0,1)$, $(0,1,1,0)$. ☐

Corollary 1. *If* $\text{psc}(\breve{z}) = 0$ *then* $\text{psc}(\breve{x}) = \text{psc}(\breve{y})$ *. If* $\text{psc}(\breve{z}) = 1$ *then* $\text{psc}(\breve{x})$ *is the opposite of* $\text{psc}(\breve{y})$ *.*

6. Linear independence and orthogonality between classes of physical quantities

The representation of a class of physical quantities in $\mathbb{Z}^7$ gives the means to study the linear independence and the orthogonality between classes of physical quantities. Consider $\breve{z} = \breve{o} + \breve{x} + \breve{y}$ and form the inner product $\breve{z} \cdot \breve{y} = \breve{o} \cdot \breve{y} + \breve{x} \cdot \breve{y} + \breve{y} \cdot \breve{y}$. The classes $[x]$ and $[y]$ are orthogonal when $\breve{x} \cdot \breve{y} = 0$. We find $\breve{z} \cdot \breve{y} = \breve{y} \cdot \breve{y}$ which shows a linear relationship between $\|\breve{z}\|_2$ and $\|\breve{y}\|_2$. So, an equation $[z] = [\kappa][x][y]$ in which the classes $[x]$ and $[y]$ are orthogonal expresses a linear relationship between $[z]$ and $[x]$ or between $[z]$ and $[y]$. We underline the difference between *linearly independent physical quantities* and *orthogonal physical quantities* [63]. From these properties we define 6 types of pairwise combinations of $[x]$ and $[y]$. We give examples of each of the types. Consider the representation of distance by the lattice point $\breve{r} = (1,0,0,0,0,0,0)$ and the representation of the linear momentum by the lattice point $\breve{p} = (1,1,-1,0,0,0,0)$. We consider the 2×7 matrix formed by the coordinates of $\breve{r}$ and $\breve{p}$ and obtain the rank = 2 for this matrix which means that $\breve{r}$ and $\breve{p}$ are *linearly independent*. For the inner product we find $\breve{r} \cdot \breve{p} = 1 \neq 0$ and so $\breve{r}$ and $\breve{p}$ are *not orthogonal*. Consider the product of length and time with representation $\breve{lt} = (1,0,1,0,0,0,0)$ and energy represented by the lattice point $\breve{E} = (2,1,-2,0,0,0,0)$, we find that $\breve{lt}$ and $\breve{E}$ are *linearly independent* and *orthogonal*. Consider the distance representation $\breve{r} = (1,0,0,0,0,0,0)$ and the wave vector representation $\breve{k} = (-1,0,0,0,0,0,0)$, we find that $\breve{r}$ and $\breve{k}$ are *linearly dependent* and *not orthogonal*. Consider the velocity representation $\breve{v} = (1,0,-1,0,0,0,0)$ and the reciprocal velocity representation $\breve{v_r} = (-1,0,1,0,0,0,0)$, we find that $\breve{v}$ and $\breve{v_r}$ are *linearly dependent* and *orthogonal*. We conclude that ternary equations $[z] = [\kappa][x][y]$ of physical quantities are only one of the six following cases:

(i) $\breve{x} \cdot \breve{y} > 0$ and 2×7 matrix rank $= 2$ (not orthogonal with positive inner product, linearly independent)

(ii) $\breve{x} \cdot \breve{y} = 0$ and 2×7 matrix rank $= 2$ (orthogonal, linearly independent)

(iii) $\breve{x} \cdot \breve{y} < 0$ and 2×7 matrix rank $= 2$ (not orthogonal with negative inner product, linearly independent)

(iv) $\breve{x} \cdot \breve{y} > 0$ and 2×7 matrix rank < 2 (not orthogonal with positive inner product, linearly dependent)

(v) $\breve{x} \cdot \breve{y} = 0$ and 2×7 matrix rank < 2 (orthogonal, linearly dependent)

(vi) $\breve{x} \cdot \breve{y} < 0$ and 2×7 matrix rank < 2 (not orthogonal with negative inner product, linearly dependent)

6.1. Decompositions of a vertex in pairwise orthogonal vertices

The decomposition of a vertex $\breve{z}$ in two pairwise orthogonal vertices $\breve{x}$ and $\breve{y}$ assumes the existence of a system of Diophantine equations:

$$\breve{x} + \breve{y} - \breve{z} = 0 \,, \tag{8a}$$

$$\breve{x} \cdot \breve{y} = 0 \,, \tag{8b}$$

where $\breve{x}, \breve{y}, \breve{z} \in \mathbb{Z}^7$. We eliminate $\breve{y}$ from the equation (8b) and find:

$$\breve{x} \cdot \breve{x} - \breve{x} \cdot \breve{z} = 0 \,. \tag{9}$$

We apply the method of "completing the square" and write equation (9) as:

$$(\breve{x} - \frac{\breve{z}}{2})^2 = (\frac{\breve{z}}{2})^2 \,, \tag{10}$$

that represents a seven-dimensional hypersphere with center at $\frac{\breve{z}}{2}$ with radius $\|\frac{\breve{z}}{2}\|_2$. We note that the hyper-surface area of a *unit* radius hypersphere reaches a *maximum* in a 7-dimensional space [64]. The center of the 7-sphere is only a lattice point of $\mathbb{Z}^7$ if all the coordinates of $\breve{z}$ are even. The solution set of the equation (10) are the integer lattice points incident on the 7-sphere and thus is a *finite* set. It is obvious that a bijection exists between the physical quantity having the vertex $\breve{z}$ and the 7-sphere with equation (10). A closed form for the solution set is not known to the author. We use the *brute force* method and list the vertices of 524287 parallelograms $\breve{o}\breve{x}\breve{z}\breve{y}$ embedded in $\mathbb{Z}^7$ representing equations $[z] = [\kappa][x][y]$. From this listing, we find parallelograms that have the property of being a rectangle. Let $n_d = \#\,(O_d)$ represent the cardinality of the set of pairwise orthogonal vertices in $\mathbb{Z}^d \times \{0\}^{7-d}$ with dimension $d \in \mathbb{N}$ where $2 \leq d \leq 7$. Table **??** contains the cardinalities of the commonly known leader classes.

Example 6.1. We solve the equation (10) for the leader class $[2^2 1 0^4]$, that represents the class *energy*. Table **??** enumerates the 60 pairs of orthogonal vertices of $\mathbb{Z}^7$ resulting in the vertex $\breve{E} = \breve{z} = (2, 1, -2, 0, 0, 0, 0)$. The orthogonality analysis of the 524287 parallelograms spans a range of perimeters from $p_p = 6$ to $p_p = 23,832$. Table 8 lists the 4 pairs having in column 1 the respective indices 1, 26, 35 and 36 that are embedded in $\mathbb{Z}^3 \times \{0\}^4$. We find that the rectangles in the 7-sphere have the perimeter values $7,657$ $8,363$ and $8,472$. The perimeter distribution indicates that the frequency of the *rectangle* perimeters is respectively 1, 17 and 26. Column 5 of Table 8 gives the 2×7 matrix rank. We observe that the 4 orthogonal pairs have rank 2 and thus are linearly independent. We find that the pair with index $Id = 1$ is the only rectangle having also frequency 1. This rectangle emphasizes the uniqueness of the form $E = \beta_1 m v^2$ that is best known as the equation $E = \gamma m_0 c^2$.

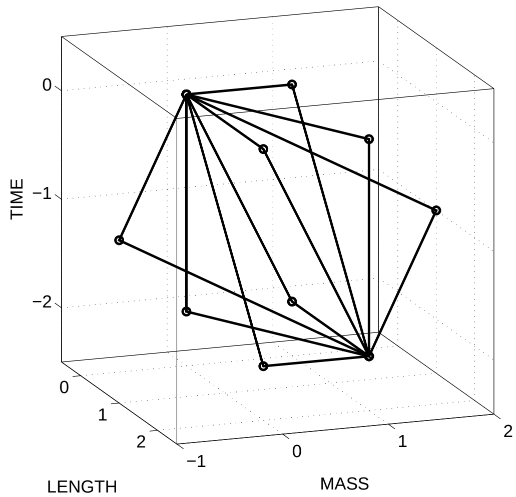

Figure 6: Rectangles embedded in $\mathbb{Z}^3 \times \{0\}^4$ representing ternary equations of *energy*

Table 8: Equations of orthogonal lattice points for *energy* in $\mathbb{Z}^3 \times \{0\}^4$.

Id	p_p	$\breve{x}$	$\breve{y}$	2×7 matrix rank	Form	Proposal
1	7,657	(0,1,0,0,0,0,0)	(2,0,-2,0,0,0,0)	2	$E = \beta_1 m v^2$	$E = \gamma m_0 c^2$
26	8,363	(1,-1,-1,0,0,0,0)	(1,2,-1,0,0,0,0)	2	$E = \beta_2 \frac{v}{m} \frac{p^2}{v}$	$E = \gamma_2 \frac{p^2}{2m}$
35	8,472	(2,1,0,0,0,0,0)	(0,0,-2,0,0,0,0)	2	$E = \beta_3 m A \nu^2$	$E = \beta_3 m x^2 \omega^2$
36	8,472	(0,1,-2,0,0,0,0)	(2,0,0,0,0,0,0)	2	$E = \beta_4 A \frac{m}{t^2}$	$E = \beta_4 A \frac{\partial^2 m}{\partial t^2}$

The 4 rectangles representing ternary *energy* equations in $\mathbb{Z}^3 \times \{0\}^4$ are shown in (Fig. 6).

7. Future work and conclusion

We construct the mathematical foundation for *the discrete geometry of physical quantities* . We prove that ternary operations between components of physical quantities are equivalent to a *parallelogram* in the integer lattice $\mathbb{Z}^7$. This equivalence is the basis for a *computer search for relations between physical quantities* based on geometric properties between the integer lattice points of $\mathbb{Z}^7$, which are the representatives of components of physical quantities. We develop an algorithm that creates a listing of the equations of the type $[z] = [\kappa][x][y]$ where $[\kappa], [x], [y], [z]$ represents components of physical quantities. We find that ternary relations between physical quantities are classified in 4 distinct 2-colouring patterns of $\mathbb{Z}^7$. Application of the algorithm for the case where $[z]$ is representing the class *energy* , results in a discrete value distribution that is characteristic for the leader class $[2^2 10^4]$. The analysis of the discrete value distribution for the physical quantity *energy* indicates the existence of *unique constellations* between physical quantities. We discover that the unique constellations representing *energy* are all embedded in a hyperplane of the integer lattice $\mathbb{Z}^7$. We observed that the frequency of some constellations is *not depending* on the dimension d of the integer lattice. The algorithm that was applied for *energy* and also for *force* is applicable to any other component of a physical quantity resulting in the discovery of new constellations between physical quantities. The compilation of the listings generated by the algorithm, will result in a catalog of equations of the type $[z] = [\kappa][x][y]$. The equivalence relation z_1 *has the same isoperimetric distribution as* z_2 applied on a finite set, representing a measure polytope of $\mathbb{Z}^7$, results in the classification of physical quantities. We show that morphisms exists between these equivalence classes and monomials. Assignment of a *Gödel number* to each physical quantity in $\mathbb{Z}^7_+$ reveals the existence of a unique *Gödel walk* in $\mathbb{Z}^k_+$. A scheme is described for analyzing n-ary operations based on the factorization of the *Gödel number* of leader class representatives in distinct integer factors, that will allow the exploration of more complex constellations than parallelograms. The n-ary operations between physical quantities are representing *paths* connecting the lattice points of the constellation representing the physical quantity under study. Orthogonality and linear independence properties of the pairs of vertices $\breve{x}$ and $\breve{y}$ result in classifying the ternary equations $[z] = [\kappa][x][y]$ in 6 distinct types. We find that each vertex $\breve{z}$ can be decomposed in a finite number of pairwise *orthogonal* vertices incident on a *unique* 7-sphere. The discrete geometry of physical quantities provides inherently a predictive property for finding the form of equations between physical quantities that are yet to be discovered. This research shows that our knowledge about the components of physical quantities and about their constellations is far from being understood and that large *hypervolumes* of $\mathbb{Z}^7$, are still to be explored. The appendices contain a preliminary classification of common physical quantities based on the measure polytopes P^s_7. The appendices also contain numerical data useful as starting point for the further exploration of the discrete geometry of physical quantities.

Acknowledgments

I thank from the University of Ghent Prof. em. F. Brackx, Prof. H. De Schepper, Assistant Prof. H. De Bie and from the University of Brussels Prof. em. I. Veretennicoff, Prof. Ph. Cara and Prof. J.P. Van Bendegem for fruitful discussions and commenting the article and Mr. B. Chevalier for the software code to calculate the isoperimetric distribution. Special thanks to my wife, children and friends for supporting me in this research.

Appendix A. 3-cycle isoperimetric distribution algorithm

Algorithm. *Calculate for each integer lattice point $\breve{x}$ of a 7-dimensional lattice the following:*

(i) $d(\breve{o}, \breve{z})$, *the Euclidean distance from $\breve{o}$ to the lattice point $\breve{z}$, representing a component of a physical quantity with coordinates* $(Z^1, \ldots, Z^7)$,

(ii) $d(\breve{x}, \breve{o})$, *the Euclidean distance from $\breve{x}$ to the origin $\breve{o}$,*

(iii) the cosine of the angle between $\breve{x}$ and $\breve{z}$,

(iv) $2a = d(\breve{z}, \breve{x}) + d(\breve{x}, \breve{o})$, *that is a characteristic of an ellipse,*

(v) the perimeter of the 3-cycle $p_t = d(\breve{o}, \breve{z}) + d(\breve{z}, \breve{x}) + d(\breve{x}, \breve{o})$,

(vi) store these results in a data structure allowing sorting by perimeter,

(vii) query the data structure to obtain the number of lattice points $\breve{x}$ generating the same triangle perimeter,

(viii) find for each triangle perimeter p_t the number of points corresponding to this triangle perimeter and record the discrete value distribution,

(ix) select the set of vertices having the same perimeter starting with the shortest 3-cycle perimeter,

(x) calculate for each of these vertices the complementary vertices and write them in adjacent rows creating a listing of increasing perimeter.

Appendix B. Algorithm for finding all the n-ary operations of a physical quantity

Algorithm. *Execute the following steps:*

(i) Identify to which class the physical quantity belongs;

(ii) apply the function "dex" on the class of the physical quantity and identify the lattice point $\breve{z}$, representing a component of a physical quantity with coordinates $(Z^1, \ldots, Z^7)$;

(iii) associate to the coordinates $(Z^1, \ldots, Z^7)$ its leader class representative;

(iv) calculate using the function $\phi_7()$ the Gödel number;

(v) if the Gödel number is ≤ 1500 then;

(vi) open lookup table OEIS A045778 and identify the row correponding to the Gödel number and record the correponding factorization;

(vii) else

(viii) perform the factorization of the Gödel number in distinct integer factors;

(ix) calculate using the inverse Gödel encoding the additive partitions of the leader class representative;

(x) apply the appropriate signed permutation to transform the leader class representative in the physical quantity under investigation;

(xi) generate a table of forms of equations for the physical quantity under study.

Appendix C. Measure polytopes

The enumeration table (Table C.9) of measure polytopes P_7^4 consists of 8 columns. The second column is the row identifier. The third column gives the representative of the leader class. The fourth column contains the sum of the absolute value of the coordinates of the lattice points being elements of the leader class that is exclusively the total degree of the monomial associated with the leader class. The fifth column gives the parity of the representative of the leader class. The sixth column gives the ℓ_1-norm of the representative. The seventh column gives the cardinality of the leader class. The eighth column gives the Gödel number of the representative. Observe that for $\|\breve{x}\|_\infty = 1$ the representative lattice points of the leader classes generate the *successive minima* R_i of the lattice $\mathbb{Z}^7$ [69]. The successive minima R_i are given in the column 6 and correspond to the values of $N(\breve{z})$, the norm of the lattice point and thus the representative lattice points of the leader classes for $s = 1$ form a set of minimal points of the lattice $\mathbb{Z}^7$ [69]. Observe that the leader class $[2^2 10^4]$ contains 840 integer lattice points with the same geometrical properties as the physical quantity *energy*. The 7×7 signed permutation matrix $\mathsf{P}_{21-2,221}$ transforms all *energy constellations* to the leader class $[2^2 10^4]$:

$$\mathsf{P}_{21-2,221} = \begin{bmatrix} 1 & 0 & 0 & 0 & 0 & 0 & 0 \\ 0 & 0 & -1 & 0 & 0 & 0 & 0 \\ 0 & 1 & 0 & 0 & 0 & 0 & 0 \\ 0 & 0 & 0 & 1 & 0 & 0 & 0 \\ 0 & 0 & 0 & 0 & 1 & 0 & 0 \\ 0 & 0 & 0 & 0 & 0 & 1 & 0 \\ 0 & 0 & 0 & 0 & 0 & 0 & 1 \end{bmatrix} \tag{C.1}$$

The representative of the leader class $[2^2 10^4]$ is a physical quantity that could be expressed as an integral of the form $\int \kappa(\lambda m_0)^2 dt$. This is the time integral of the square of the quantity with lattice point (1,1,0,0,0,0,0).

Table C.9: Partitions of the measure polytope P_7^4

$\|\breve{x}\|_\infty = s$	Id	leader class	deg	psc $(\breve{z})$	$N(\breve{z})$	Number of vertices	Gödel number
0	1	$[0^7]$	0	0	0	1	1
1	1	$[10^6]$	1	1	1	14	2
1	2	$[1^2 0^5]$	2	0	2	84	6
1	3	$[1^3 0^4]$	3	1	3	280	30
1	4	$[1^4 0^3]$	4	0	4	560	210
1	5	$[1^5 0^2]$	5	1	5	672	2310
1	6	$[1^6 0]$	6	0	6	448	30030
1	7	$[1^7]$	7	1	7	128	510510
2	1	$[20^6]$	2	0	4	14	4
2	2	$[210^5]$	3	1	5	168	12
2	3	$[21^2 0^4]$	4	0	6	840	60
2	4	$[2^2 0^5]$	4	0	8	84	36
2	5	$[21^3 0^3]$	5	1	7	2240	420
2	6	$[2^2 10^4]$	5	1	9	840	180
2	7	$[21^4 0^2]$	6	0	8	3360	4620
2	8	$[2^2 1^2 0^3]$	6	0	10	3360	1260
2	9	$[2^3 0^4]$	6	0	12	280	900
2	10	$[21^5 0]$	7	1	9	2688	60060
2	11	$[2^2 1^3 0^2]$	7	1	11	6720	13860
2	12	$[2^3 10^3]$	7	1	13	2240	6300
2	13	$[21^6]$	8	0	10	896	1021020
2	14	$[2^2 1^4 0]$	8	0	12	6720	180180
2	15	$[2^3 1^2 0^2]$	8	0	14	6720	69300
2	16	$[2^4 0^3]$	8	0	16	560	44100
...	...	...	...	...	...	...	...

$\|\check{x}\|_\infty = s$	Id	leader class	deg	psc $(\check{z})$	$N(\check{z})$	Number of vertices	Gödel number
2	17	$[2^2 1^5]$	9	1	13	2688	3063060
2	18	$[2^3 1^3 0]$	9	1	15	8960	900900
2	19	$[2^4 1 0^2]$	9	1	17	3360	485100
2	20	$[2^3 1^4]$	10	0	16	4480	15315300
2	21	$[2^4 1^2 0]$	10	0	18	6720	6306300
2	22	$[2^5 0^2]$	10	0	20	672	5336100
2	23	$[2^4 1^3]$	11	1	19	4480	107207100
2	24	$[2^5 1 0]$	11	1	21	2688	69369300
2	25	$[2^5 1^2]$	12	0	22	2688	1179278100
2	26	$[2^6 0]$	12	0	24	448	901800900
2	27	$[2^6 1]$	13	1	25	896	15330615300
2	28	$[2^7]$	14	0	28	128	260620460100
3	1	$[3 0^6]$	3	1	9	14	8
3	2	$[3 1 0^5]$	4	0	10	168	24
3	3	$[3 1^2 0^4]$	5	1	11	840	120
3	4	$[3 2 0^5]$	5	1	13	168	72
3	5	$[3 1^3 0^3]$	6	0	12	2240	840
3	6	$[3 2 1 0^4]$	6	0	14	1680	360
3	7	$[3^2 0^5]$	6	0	18	84	216
3	8	$[3 1^4 0^2]$	7	1	13	3360	9240
3	9	$[3 2 1^2 0^3]$	7	1	15	6720	2520
3	10	$[3 2^2 0^4]$	7	1	17	840	1800
3	11	$[3^2 1 0^4]$	7	1	19	840	1080
3	12	$[3 1^5 0]$	8	0	14	2688	120120
3	13	$[3 2 1^3 0^2]$	8	0	16	13440	27720
3	14	$[3 2^2 1 0^3]$	8	0	18	6720	12600
3	15	$[3^2 1^2 0^3]$	8	0	20	3360	7560
3	16	$[3^2 2 0^4]$	8	0	22	840	5400
3	17	$[3 1^6]$	9	1	15	896	2042040
3	18	$[3 2 1^4 0]$	9	1	17	13440	360360
3	19	$[3 2^2 1^2 0^2]$	9	1	19	20160	138600
3	20	$[3 2^3 0^3]$	9	1	21	2240	88200
3	21	$[3^2 1^3 0^2]$	9	1	21	6720	83160
3	22	$[3^2 2 1 0^3]$	9	1	23	6720	37800
3	23	$[3^3 0^4]$	9	1	27	280	27000
3	24	$[3 2 1^5]$	10	0	18	5376	6126120
3	25	$[3 2^2 1^3 0]$	10	0	20	26880	1801800
3	26	$[3 2^3 1 0^2]$	10	0	22	13440	970200
3	27	$[3^2 1^4 0]$	10	0	22	6720	1081080
3	28	$[3^2 2 1^2 0^2]$	10	0	24	20160	415800
3	29	$[3^2 2^2 0^3]$	10	0	26	3360	264600
3	30	$[3^3 1 0^3]$	10	0	28	2240	189000
3	31	$[3 2^2 1^4]$	11	1	21	13440	30630600
3	32	$[3 2^3 1^2 0]$	11	1	23	26880	12612600
3	33	$[3 2^4 0^2]$	11	1	25	3360	10672200
3	34	$[3^2 1^5]$	11	1	23	2688	18378360
3	35	$[3^2 2 1^3 0]$	11	1	25	26880	5405400
...	...	...	...	...	...	...	...

$\|\check{x}\|_\infty = s$	Id	leader class	deg	psc $(\check{z})$	$N(\check{z})$	Number of vertices	Gödel number
3	36	$[3^2 2^2 1 0^2]$	11	1	27	20160	2910600
3	37	$[3^3 1^2 0^2]$	11	1	29	6720	2079000
3	38	$[3^3 2 0^3]$	11	1	31	2240	1323000
3	39	$[3 2^3 1^3]$	12	0	24	17920	214414200
3	40	$[3 2^4 1 0]$	12	0	26	13440	138738600
3	41	$[3^2 2 1^4]$	12	0	26	13440	91891800
3	42	$[3^2 2^2 1^2 0]$	12	0	28	40320	37837800
3	43	$[3^2 2^3 0^2]$	12	0	30	6720	32016600
3	44	$[3^3 1^3 0]$	12	0	30	8960	27027000
3	45	$[3^3 2 1 0^2]$	12	0	32	13440	14553000
3	46	$[3^4 0^3]$	12	0	36	560	9261000
3	47	$[3 2^4 1^2]$	13	1	27	13440	2358556200
3	48	$[3 2^5 0]$	13	1	29	2688	1803601800
3	49	$[3^2 2^2 1^3]$	13	1	29	26880	643242600
3	50	$[3^2 2^3 1 0]$	13	1	31	26880	416215800
3	51	$[3^3 1^4]$	13	1	31	4480	459459000
3	52	$[3^3 2 1^2 0]$	13	1	33	26880	189189000
3	53	$[3^3 2^2 0^2]$	13	1	35	6720	160083000
3	54	$[3^4 1 0^2]$	13	1	37	3360	101871000
3	55	$[3 2^5 1]$	14	0	30	5376	30661260600
3	56	$[3^2 2^3 1^2]$	14	0	32	26880	7075668600
3	57	$[3^2 2^4 0]$	14	0	34	6720	5410805400
3	58	$[3^3 2 1^3]$	14	0	34	17920	3216213000
3	59	$[3^3 2^2 1 0]$	14	0	36	26880	2081079000
3	60	$[3^4 1^2 0]$	14	0	38	6720	1324323000
3	61	$[3^4 2 0^2]$	14	0	40	3360	1120581000
3	62	$[3 2^6]$	15	1	33	896	521240920200
3	63	$[3^2 2^4 1]$	15	1	35	13440	91983691800
3	64	$[3^3 2^2 1^2]$	15	1	37	26880	35378343000
3	65	$[3^3 2^3 0]$	15	1	39	8960	27054027000
3	66	$[3^4 1^3]$	15	1	39	4480	22513491000
3	67	$[3^4 2 1 0]$	15	1	41	13440	14567553000
3	68	$[3^5 0^2]$	15	1	45	672	12326391000
3	69	$[3^2 2^5]$	16	0	38	2688	1563722760600
3	70	$[3^3 2^3 1]$	16	0	40	17920	459918459000
3	71	$[3^4 2 1^2]$	16	0	42	13440	247648401000
3	72	$[3^4 2^2 0]$	16	0	44	6720	189378189000
3	73	$[3^5 1 0]$	16	0	46	2688	160243083000
3	74	$[3^3 2^4]$	17	1	43	4480	7818613803000
3	75	$[3^4 2^2 1]$	17	1	45	13440	3219429213000
3	76	$[3^5 1^2]$	17	1	47	2688	2724132411000
3	77	$[3^5 2 0]$	17	1	49	2688	2083160079000
3	78	$[3^4 2^3]$	18	0	48	4480	54730296621000
3	79	$[3^5 2 1]$	18	0	50	5376	35413721343000
3	80	$[3^6 0]$	18	0	54	448	27081081027000
3	81	$[3^5 2^2]$	19	1	53	2688	602033262831000
3	82	$[3^6 1]$	19	1	55	896	460378377459000
...	...	...	...	...	...	...	...

$\|\check{x}\|_\infty = s$	Id	leader class	deg	psc $(\check{z})$	$N(\check{z})$	Number of vertices	Gödel number
3	83	$[3^62]$	20	0	58	896	7826432416803000
3	84	$[3^7]$	21	1	63	128	133049351085651000

Appendix D. Relation between 7-spheres and the leader classes of measure polytopes

Table D.10: Partitioning 7-spheres in leader classes of measure polytopes

N	disjunct union of leader classes of measure polytopes	$r_7(N)$
0	$[0^7]$	1
1	$[10^6]$	14
2	$[1^20^5]$	84
3	$[1^30^4]$	280
4	$[1^40^3] \cup [20^6]$	574
5	$[1^50^2] \cup [210^5]$	840
6	$[1^60] \cup [21^20^4]$	1288
7	$[1^7] \cup [21^30^3]$	2368
8	$[2^20^5] \cup [21^40^2]$	3444
9	$[2^210^4] \cup [21^50] \cup [30^6]$	3542
10	$[2^21^20^3] \cup [21^6] \cup [310^5]$	4424
11	$[2^21^30^2] \cup [31^20^4]$	7560
12	$[2^30^4] \cup [2^21^40] \cup [31^30^3]$	9240
13	$[2^310^3] \cup [2^21^5] \cup [320^5] \cup [31^40^2]$	8456
14	$[2^31^20^2] \cup [3210^4] \cup [31^50]$	11088
15	$[2^31^30] \cup [321^20^3] \cup [31^6]$	16576
16	$[2^40^3] \cup [2^31^4] \cup [321^30^2] \cup [40^6]$	18494
17	$[2^410^2] \cup [32^20^4] \cup [321^40] \cup [410^5]$	17808
18	$[2^41^20] \cup [3^20^5] \cup [32^210^3] \cup [321^5] \cup [41^20^4]$	19740
19	$[2^41^3] \cup [3^210^4] \cup [32^21^20^2] \cup [41^30^3]$	27720
20	$[2^50^2] \cup [3^21^20^3] \cup [32^21^30] \cup [41^40^2] \cup [420^5]$	34440
21	$[2^510] \cup [32^30^3] \cup [3^21^30^2] \cup [32^21^4] \cup [41^50] \cup [4210^4]$	29456
22	$[2^51^2] \cup [3^220^4] \cup [32^310^2] \cup [3^21^40] \cup [41^6] \cup [421^20^3]$	31304
23	$[3^2210^3] \cup [32^31^20] \cup [3^21^5] \cup [421^30^2]$	49728
24	$[2^60] \cup [3^221^20^2] \cup [32^31^3] \cup [421^40] \cup [42^20^4]$	52808
25	$[2^61] \cup [32^40^2] \cup [3^221^30] \cup [421^5] \cup [42^210^3] \cup [430^5] \cup [50^6]$	43414
26	$[3^22^20^3] \cup [32^410] \cup [3^221^4] \cup [42^21^20^2] \cup [4310^4] \cup [510^5]$	52248
27	$[3^30^4] \cup [3^22^210^2] \cup [32^41^2] \cup [42^21^30] \cup [431^20^3] \cup [51^20^4]$	68320
28	$[2^7] \cup [3^310^3] \cup [3^22^21^20] \cup [42^21^4] \cup [42^30^3] \cup [431^30^2] \cup [51^30^3]$	74048
29	$[3^31^20^2] \cup [32^50] \cup [3^22^21^3] \cup [42^310^2] \cup [431^40] \cup [4320^4] \cup [51^40^2] \cup [520^5]$	68376
30	$[3^22^30^2] \cup [3^31^30] \cup [32^51] \cup [42^31^20] \cup [431^5] \cup [43210^3] \cup [51^50] \cup [5210^4]$	71120
31	$[3^320^3] \cup [3^22^310] \cup [3^31^4] \cup [42^31^3] \cup [4321^20^2] \cup [51^6] \cup [521^20^3]$	99456
32	$[3^3210^2] \cup [3^22^31^2] \cup [42^40^2] \cup [4^20^5] \cup [4321^30] \cup [521^30^2]$	110964
33	$[3^321^20] \cup [32^6] \cup [42^410] \cup [4^210^4] \cup [4321^4] \cup [432^20^3] \cup [521^40] \cup [52^20^4]$	89936
34	$[3^22^40] \cup [3^321^3] \cup [42^41^2] \cup [432^210^2] \cup [43^20^4] \cup [4^21^20^3] \cup [521^5] \cup [52^210^3] \cup [530^5]$	94864
35	$[3^32^20^2] \cup [3^22^41] \cup [43^210^3] \cup [4^21^30^2] \cup [432^21^20] \cup [52^21^20^2] \cup [5310^4]$	136080

Appendix E. Isoperimetric distributions of classes of the first polytope shell

Table E.11 consists of 8 columns and represents the isoperimetric distributions of leader classes of polytope shell $P_7^1 \setminus P_7^0$. The first column is the index of the integer sequence of frequencies of the respective isoperimetric distributions. The other columns contain each the first 50 frequencies of the isoperimetric distribution corresponding to the leader classes containing known physical quantities from the measure polytope P_7^1 . Study of the minimum frequencies f_{min} in the 7 distributions and the corresponding vertices results in finding the classes that have *unique* ternary operations. The results for the measure polytope P_7^1 are that *only* leader class 2 contains *unique* parallelograms. The ternary operation for leader class 2 is represented by a physical quantity that is expressed as $length \times mass$. Observe that the frequencies in the sequence of leader class 1 also appear in the OEIS [40] sequence A000141 given by $r_6(m) = 1, 12, 60, 160, 252, 312, 544, 960 \ldots$. The sequence represents the number of ways of writing a positive integer m as a sum of *six* integral squares. It is known that this OEIS sequence A000141 is related to the theta function [56].

Table E.11: Truncated ($n \leq 50$) integer sequences of the frequencies of the isoperimetric distributions of leader classes of the measure polytope $P_7^1 \setminus P_7^0$.

n	$cl1$	$cl2$	$cl3$	$cl4$	$cl5$	$cl6$	$cl7$
1	1	1	1	1	1	1	1
2	12	1	3	4	5	6	7
3	1	10	8	3	10	15	21
4	60	10	24	6	4	10	35
5	12	2	3	24	20	2	7
6	160	42	30	18	40	12	42
7	60	40	75	4	5	30	105
8	252	20	24	24	24	26	147
9	160	100	80	60	50	30	147
10	312	80	120	40	65	60	21
11	1	1	3	24	20	66	105
12	252	80	75	80	80	30	210
13	544	170	168	104	120	12	252
14	12	91	150	48	100	60	315
15	312	10	24	6	10	120	441
16	960	160	120	60	50	15	35
17	60	272	240	156	114	132	147
18	544	122	288	180	170	60	252
19	1020	42	1	78	200	60	350
20	160	182	75	36	40	92	595
21	960	420	150	104	120	102	735
22	876	280	246	156	128	165	574
23	252	100	504	264	160	110	35
24	1020	244	8	176	10	30	147
25	1560	544	120	4	320	120	315
26	312	400	288	80	65	180	595
27	876	2	400	180	170	20	882
28	2400	170	528	192	260	180	840
29	1	560	30	328	320	270	854
...	...	...	...	...	...	...	...

n	$cl1$	$cl2$	$cl3$	$cl4$	$cl5$	$cl6$	$cl7$
30	544	682	150	240	375	180	1260
31	1560	290	504	24	40	66	21
32	2080	20	750	96	100	102	147
33	12	272	510	264	160	200	441
34	960	800	80	480	400	360	735
35	2400	910	288	480	5	342	840
36	2040	362	528	193	560	166	1050
37	60	80	728	60	340	132	1575
38	1020	420	840	156	65	180	1785
39	2080	580	3	328	200	15	1470
40	3264	1040	168	636	320	280	7
41	160	800	504	624	424	480	147
42	876	160	510	219	520	420	441
43	2040	544	576	6	20	132	574
44	4160	724	1227	104	530	60	854
45	252	1220	24	352	100	165	1575
46	1560	880	240	480	320	360	1750
47	3264	1	528	438	560	450	1533
48	4092	182	840	680	1	30	1932
49	312	682	1200	468	484	390	2387
50	2400	1600	1200	24	500	570	1

Appendix F. Isoperimetric distributions of leader classes of the second polytope shell

Table F.12 consists of 11 columns and represents the isoperimetric distributions of leader classes of polytope shell $P_7^2 \setminus P_7^1$. The first column is the index of the integer sequence of frequencies of the respective isoperimetric distributions. The other columns contain each the first 50 frequencies of the isoperimetric distribution corresponding to the leader classes with $s = 2$ and respective Id from the measure polytope P_7^3. Observe that minimum frequencies $f_{min} = 1$ are present in the distributions. Listing the vertices that correspond to those frequency minima results in finding the leader classes that have *unique* ternary operations. The leader class with $s = 2$ and $Id = 6$ (see C.9) has been studied in detail.

Table F.12: Truncated ($n \leq 50$) integer sequences of the frequencies of the isoperimetric distributions of leader classes of the polytope shell $P_7^2 \setminus P_7^1$.

n	$cl1$	$cl2$	$cl3$	$cl4$	$cl5$	$cl6$	$cl7$	$cl8$	$cl11$	$cl12$
1	1	1	1	2	1	1	1	1	1	1
2	6	1	1	2	1	1	1	1	1	1
3	12	1	1	5	3	2	4	1	3	3
4	30	10	2	20	3	2	3	2	2	3
5	60	10	9	31	9	8	4	4	6	3
6	81	11	8	80	19	1	10	8	3	6
7	160	40	8	50	6	16	20	8	10	3
8	126	1	18	42	21	8	17	13	14	1
...	...	...	...	...	...	...	...	...	...	...

n	$cl1$	$cl2$	$cl3$	$cl4$	$cl5$	$cl6$	$cl7$	$cl8$	$cl11$	$cl12$
9	12	40	34	2	3	17	20	6	11	18
10	252	1	26	160	36	26	4	26	4	19
11	156	50	26	85	45	10	40	28	28	18
12	60	81	1	100	18	1	44	14	36	18
13	312	11	64	20	1	48	20	16	29	6
14	272	80	74	182	57	56	16	2	18	21
15	160	120	34	136	83	50	1	34	3	40
16	544	100	18	170	63	26	44	60	32	9
17	480	10	50	80	21	2	80	2	48	45
18	252	50	112	244	50	42	20	16	12	47
19	960	90	9	211	82	65	80	60	62	39
20	511	1	120	272	9	10	32	24	62	3
21	312	170	41	560	120	90	60	52	45	18
22	1020	152	64	432	122	88	10	16	18	57
23	438	40	2	10	57	48	80	57	72	45
24	12	120	88	420	3	16	91	62	57	60
25	544	114	114	800	114	96	140	98	75	36
26	876	202	185	341	108	58	88	55	44	96
27	780	10	104	182	135	98	44	36	132	9
28	60	320	34	42	36	42	4	13	11	43
29	960	81	112	544	249	160	106	88	68	81
30	1560	170	164	580	82	2	140	100	106	44
31	1200	260	16	455	150	72	40	52	45	78
32	160	352	164	244	19	136	122	84	134	18
33	1020	411	264	100	210	48	184	144	6	104
34	2400	40	184	682	219	139	130	98	140	111
35	1040	100	74	724	276	1	80	82	160	83
36	252	202	114	520	83	184	96	94	96	36
37	876	400	1	560	3	208	20	34	32	66
38	2080	1	240	910	108	96	184	1	93	3
39	1020	560	368	170	150	17	280	166	1	102
40	312	322	330	1600	339	116	244	234	105	172
41	1560	81	194	610	45	162	176	201	228	78
42	2040	152	120	2	399	296	6	170	68	210
43	1632	352	164	800	246	65	140	26	251	108
44	544	360	9	1040	120	352	160	136	147	39
45	2400	520	304	272	210	212	44	128	28	3
46	3264	11	480	272	19	8	244	57	116	120
47	2081	530	427	1760	300	136	400	212	162	153
48	960	100	160	850	366	176	364	324	72	83
49	2080	320	68	20	435	56	128	8	194	192
50	4160	560	185	580	63	256	91	262	10	21

Appendix G. Isoperimetric distributions of leader classes of the third polytope shell

Table G.13 consists of 11 columns and represents the isoperimetric distributions of leader classes of polytope shell $P_7^3 \setminus P_7^2$. The first column is the index of the integer sequence of frequencies of the respective isoperimetric distributions. The other columns contain each the first 50 frequencies of the isoperimetric distribution corresponding to the leader classes with $s = 3$ and respective Id from the measure polytope P_7^3. Observe that minimum frequencies $f_{min} = 1$ are present in the distributions. Listing the vertices that correspond to those frequency minima results in finding the leader classes that have *unique* ternary operations.

Table G.13: Truncated ($n \leq 50$) integer sequences of the frequencies of the isoperimetric distributions of leader classes of the polytope shell $P_7^3 \setminus P_7^2$.

n	$cl1$	$cl2$	$cl3$	$cl4$	$cl5$	$cl6$	$cl9$	$cl14$	$cl15$	$cl22$
1	2	1	1	1	1	1	1	1	1	1
2	12	1	1	1	1	1	1	1	1	1
3	12	1	2	1	3	1	1	1	2	1
4	60	10	1	1	3	1	2	2	1	1
5	160	10	8	10	1	1	1	1	2	2
6	60	1	2	1	6	1	2	2	2	1
7	1	1	16	10	3	8	1	6	2	2
8	252	10	8	40	18	9	7	2	6	2
9	160	40	3	10	18	1	13	2	4	6
10	312	40	8	10	6	9	9	8	12	8
11	12	1	26	10	6	1	8	2	6	3
12	252	10	48	40	6	9	2	13	12	1
13	544	10	28	1	19	24	15	1	12	8
14	60	10	16	1	39	8	26	8	4	13
15	312	80	2	80	3	9	9	14	2	13
16	960	40	24	40	18	32	30	15	12	2
17	544	80	48	40	42	9	34	26	16	7
18	160	10	26	1	18	32	26	13	28	1
19	1020	40	64	40	36	1	2	14	6	14
20	960	1	64	80	18	10	15	6	24	13
21	252	10	49	11	50	33	43	13	20	26
22	876	41	1	90	42	35	38	30	30	13
23	1020	90	16	1	60	57	35	38	29	21
24	1	90	74	10	44	32	1	1	24	30
25	312	40	74	80	42	33	34	27	2	26
26	1560	80	51	1	1	1	70	32	32	6
27	876	1	48	80	18	24	14	46	28	15
28	12	80	120	90	78	56	46	40	12	22
29	544	90	3	80	96	66	1	40	40	8
30	2400	40	72	50	44	1	61	2	56	25
31	1560	112	112	10	66	40	43	32	52	1
32	2080	112	49	112	99	25	78	32	65	45
33	960	90	128	90	84	25	15	14	30	31
34	60	90	8	40	60	64	66	57	16	56
35	2400	91	120	10	84	66	90	80	56	33
36	2040	10	176	90	42	65	70	60	62	30
37	1020	1	72	10	6	57	26	82	2	9
38	160	130	24	112	116	34	62	39	40	44
...	...	...	...	...	...	...	...	...	...	...

n	$cl1$	$cl2$	$cl3$	$cl4$	$cl5$	$cl6$	$cl7$	$cl8$	$cl11$	$cl12$
39	2080	240	76	120	168	9	9	10	64	1
40	3264	241	2	90	174	96	71	68	106	50
41	876	170	122	240	152	128	143	50	12	43
42	252	40	192	113	36	97	61	44	30	62
43	2040	112	72	40	3	136	164	84	90	14
44	4160	122	267	81	99	40	103	132	17	28
45	1560	41	194	112	120	9	43	13	38	52
46	312	192	26	40	60	88	8	24	80	75
47	3264	320	112	240	145	83	90	92	64	2
48	4092	10	160	1	240	40	108	40	5	39
49	2400	330	74	40	19	152	66	60	104	53
50	544	112	224	170	225	216	146	100	32	48

References

[1] J. L. Casti, Reality Rules: Picturing the World in Mathematics, John Wiley & Sons, New York Chichester Brisbane Toronto Singapore, 1992.

[2] J.-Ph. Uzan, B. Leclercq, The Natural Laws of the Universe: Understanding Fundamental Constants, Springer-Praxis, Chichester, 2008.

[3] E.P. Wigner, Events, Laws of Nature, and Invariance Principles, Nobel Lecture, 1963.

[4] E.P. Wigner, Symmetry and Conservation Laws, Phys. Today 17 (1964) (3) 34–40.

[5] A. Einstein, Zur Elektrodynamik bewegter Körper, Annalen der Physik 17 (1905) 891–921.

[6] R.P. Feynman, The character of physical law, Twelfth printing, The M.I.T. Press, Cambridge, 1985.

[7] R.P. Feynman, The Development of the Space-Time View of Quantum Electrodynamics, Phys. Today 19 (1966) (8) 31–44.

[8] M. Tegmark, Is "the theory of everything" merely the ultimate ensemble theory?, Ann. Phys. 270 (1998) 1–51.

[9] M. Tegmark, The Mathematical Universe, Found. Phys. 36 (2006) 765–794.

[10] M. Lange, Must the Fundamental Laws of Physics be Complete?, Philosophy and Phenomenological Research 78 (2009) 312–345.

[11] J.D. Barrow, Gödel and Physics, [Internet]. [cited 23 Aug 2012]. Available from http://arXiv:physics/0612253v2 ,16 May 2007.

[12] D. Rickles, Symmetry, Structure and Spacetime, Elsevier, Amsterdam, 2008. Chapter 1, Interpretation and Formalism, 11–15.

[13] PIRSA-C10001 Laws of Nature: Their Nature and Knowability. [cited 2011 Oct 28]. Available from: http://pirsa.org/C10001.

[14] D. Rickles, Symmetry, Structure and Spacetime, Elsevier, Amsterdam, 2008. Chapter 4, Spacetime in General Relativity, 73–87.

[15] D. Rickles, Symmetry, Structure and Spacetime, Elsevier, Amsterdam, 2008. Chapter 1, Interpretation and Formalism, 1–10.

[16] F. Wilczek, On Absolute Units, I: Choices, Phys. Today 58 (2005) (10) 12–13.

[17] F. Wilczek, On Absolute Units, II: Challenges and Responses, Phys. Today 59 (2006) (1) 10–11.

[18] F. Wilczek, On Absolute Units, III: Absolutely Not?, Phys. Today 59 (2006) (5) 10–11.

[19] J.-Ph. Uzan, B. Leclercq, The Natural Laws of the Universe: Understanding Fundamental Constants, Springer-Praxis, Chichester, 2008. Chapter 4, Proportions: dimensionless parameters, 59–70.

[20] M.J. Duff, L.B. Okun, G. Veneziano, Trialogue on the number of fundamental constants, JHEP03 (2002) 023 1–30.

[21] J.J. Roche, The Mathematics of Measurement: a Critical History, The Athlone Press, London, 1998. Chapter 11, Dimensional exploration, 208–218.

[22] D. Hilbert, S. Cohn-Vossen, Geometry and the Imagination, Translated by P. Nemenyi, AMS Chelsea Publishing, Providence, 1999.

[23] J.C. Maxwell, On the Mathematical Classification of Physical Quantities, Proceedings of the London Mathematical Society Vol. III (1874) (34) 258–266.

[24] J. Schwinger, The algebra of microscopic measurement, Proc. N.A.S. 45 (1959) (10) 1542–1553.

[25] G.D. Forney, G. Ungerboeck, Modulation and Coding for Linear Gaussian Channels, IEEE Trans. Inform. Theory, 44 (1998) (6) 2384–2415.

[26] S. Lipschutz, Theory and Problems of Linear Algebra, McGraw-Hill book company, New York, 1968.

[27] H.S.M. Coxeter, Regular Polytopes, Third Edition, Dover Publications, New York, 1973. Chapter10, Forms, Vectors, and Coordinates, 178–183.

[28] BIPM, International vocabulary of metrology - Basic and general concepts and associated terms(VIM), JCGM 200:2008.

[29] J.H. Conway, N.J.A. Sloane, Sphere Packings, Lattices and Groups, Third Edition, Springer-Verlag, Berlin Heidelberg New York, 1999. Chapter 4, Certain Important Lattices and Their Properties, 106–108.

[30] R.J. Webster, Convexity, Oxford University Press, Oxford, 2002. Chapter 1, The Euclidean space $\mathbb{R}^n$, 27.

[31] J.H. Conway, N.J.A. Sloane, Sphere Packings, Lattices and Groups, Third Edition, Springer-Verlag, Berlin Heidelberg New York, 1999. Chapter 4, Certain Important Lattices and Their Properties, 94–99.

[32] R. Carter, Lie Algebras of Finite and Affine Type, Cambridge University Press, Cambridge, 2005. Chapter 8, The simple Lie algebras, 128–132.

[33] R. Diestel, Graph Theory, Second Edition, Springer-Verlag, New York, 2000. Chapter 1, The Basics, 1–12.

[34] S.V.Gervacio, I.B. Jos, The Euclidean dimension of the join of two cycles, Discrete Math. 308 (2008) 5722–5726.

[35] W.A. Coppel, Number Theory, An Introduction to Mathematics, Second Edition, Springer Science+Business Media, New York, 2009. Chapter 8, The Geometry of Numbers, 349–350.

[36] L.G. Kaya, Hybrid Approaches to Scheduling and Clustering, ProQuest LLC, Ann Arbor, 2009, Chapter 1, The Circuit Polytope, 1–6.

[37] Ch. Audet, P. Hansen, F. Messine, Extremal problems for convex polygons, J. Glob. Optim. 38 (2007) 163–179.

[38] N.C. Barford, Experimental Measurements: Precision, Error and Truth, 2nd edition, John Wiley & Sons, Chichester New York Brisbane Toronto Singapore, 1990.

[39] Abramowitz, M.,Stegun, I.A.: Handbook of Mathematical Functions, with formulas, graphs, and mathematical tables, Dover Publications, New York 1972.

[40] OEIS Foundation Inc. (2011), The On-Line Encyclopedia of Integer Sequences, [Internet].[cited 14 Jun 2011]. Available from: http://oeis.org.

[41] D. Cox, J. Little, D. O'Shea, Ideals, Varieties, and Algorithms, An Introduction to Computational Algebraic Geometry and Commutative Algebra, Third Edition, Springer Science+Business Media, New York, 2007. Chapter1; Geometry, Algebra and Algorithms, 1–48.

[42] F. Wilczek, Whence the Force of F=ma? I: Culture Shock, Phys. Today 57 (2004) (10) 11–12.

[43] F. Wilczek, Whence the Force of F=ma? II: Rationalizations, Phys. Today 57 (2004) (12) 10–11.

[44] F. Wilczek, Whence the Force of F=ma? III: Cultural Diversity, Phys. Today 58 (2005) (7) 10–11.

[45] J.H. Conway, N.J.A. Sloane, Sphere Packings, Lattices and Groups, Third Edition, Springer-Verlag, Berlin Heidelberg New York, 1999. Chapter 3, Codes, Designs and Groups, 90–93.

[46] D. Rickles, Symmetry, Structure and Spacetime, Elsevier, Amsterdam, 2008. Chapter 9, Structuralism and Symmetry, 204–205.

[47] P. Rault, Ch. Guillemot, Indexing Algorithms for Z_n, A_n, D_n, and D_n^{++} Lattice Vector Quantizers, IEEE Trans. on Multimedia 3 (2001) (4) 395–404.

[48] A. Vasilache, B. Dumitrescu, I. Tăbuş, Multiple-scale Leader-lattice VQ with application to LSF quantization, Signal Processing 82 (2002) 563–586.

[49] A. Vasilache, Tăbuş, Robust indexing of lattices and permutation codes over binary symmetric channels, Signal Processing 83 (2003) 1467–1486.

[50] S. Lipschutz, Theory and Problems of Set Theory and Related Problems, McGraw-Hill book company, New York, 1964.

[51] B. Grünbaum, Convex Polytopes, Second Edition, Springer-Verlag, New York, 2003.

[52] G.M. Ziegler, Lectures on Polytopes, Updated Seventh Printing of the First Edition, Springer Science+Business Media, New York, 2006.

[53] M. Deza, V. Grishukhin, M. Shtogrin, Scale-Isometric Polytopal Graphs in Hypercubes and Cubic Lattices: Polytopes in Hypercubes and Z_n, Imperial College Press, Singapore, 2004.

[54] D. Cox, J. Little, D. O'Shea, Ideals, Varieties, and Algorithms, An Introduction to Computational Algebraic Geometry and Commutative Algebra, Third Edition, Springer Science+Business Media, New York, 2007. Chapter 2, Groebner Bases, 54–61.

[55] D. Cox, J. Little, D. O'Shea, Ideals, Varieties, and Algorithms, An Introduction to Computational Algebraic Geometry and Commutative Algebra, Third Edition, Springer Science+Business Media, New York, 2007. Chapter 9; The Dimension of a Variety, 449.

[56] J.H. Conway, N.J.A. Sloane, Sphere Packings, Lattices and Groups, Third Edition, Springer-Verlag, Berlin Heidelberg New York, 1999. Chapter 2, Coverings, Lattices and Quantizers, 44–50.

[57] S. Feferman et al., Kurt Gödel Collected Works Volume 1 Publications 12929-1936, Oxford University Press, New York, Clarendon Press Oxford, 1986. On undecidable propositions of formal mathematical systems, p355

[58] T.M. Apostol, Introduction to Analytic Number Theory, Springer Science+Business Media, New York, 1976. Chapter 1.

[59] G. Quattrocchi, Colouring 4-cycle systems with specified block colour patterns: the case of embedding P_3-designs, Electron. J. of Combin. 8 (2001) R24.

[60] L. Gionfriddo, M. Gionfriddo, Giorgio Ragusa, Equitable specialized block-colourings for 4-cycle systems - I, Discrete Math. 310 (2010) 3126–3131.

[61] M. Gionfriddo, Giorgio Ragusa, Equitable specialized block-colourings for 4-cycle systems - II, Discrete Math. 310 (2010) 1986–1994.

[62] S.S. Epp, Discrete Mathematics with Applications, PWS Publishing Company, Boston, 1990.

[63] J.L. Rodgers, W.A. Nicewander, L. Toothaker, Linearly Independent, Orthogonal, and Uncorrelated Variables, The American Statistician 38 (1984) (2), 133 – 134.

[64] E.W. Weisstein, Hypersphere, in MathWorld - A Wolfram Web Resource, [cited 2012 Mar 08]. Available from: http://mathworld.wolfram.com/Hypersphere.html.

[65] M. Paty, Are quantum systems physical objects with physical properties?, Eur.J.Phys. 20 (1999) 373–388.

[66] J.-Ph. Uzan, B. Leclercq, The Natural Laws of the Universe: Understanding Fundamental Constants, Springer-Praxis, Chichester, 2008. Chapter 3, Planning the edifice: structure of theories, 56–58.

[67] L.B. Okun, The fundamental constants of physics, Sov. Phys. Usp. 34 (1991) (9) 818–826.

[68] J.-Ph. Uzan, B. Leclercq, The Natural Laws of the Universe: Understanding Fundamental Constants, Springer-Praxis, Chichester, 2008. Chapter 4, Proportions: dimensionless parameters, 64–65.

[69] H. Davenport, Analytic Methods for Diophantine Equations and Diophantine Inequalities, Second edition, Cambridge University Press, Cambridge, 2005.